· Article · Advances in Polar Science
doi: 10.12429/j.advps.2024.0018 September 2024 Vol. 35 No. 3: 327-369

# Distributions of dissolved oxygen and apparent oxygen utilization in the Cosmonaut Sea and Amundsen Sea in austral summer 2022

DING Yufei[1,2], ZHU Changfeng[1,2], ZHANG Cai[1,2], ZHANG Haifeng[1,2], ZHAO Jun[1,2*], GUO Xiaoze[3], ZHANG Wei[1,2] & PAN Jianming[1,2*]

[1] Key Laboratory of Marine Ecosystem Dynamics, Ministry of Natural Resources, Hangzhou 310012, China;
[2] Second Institute of Oceanography, Ministry of Natural Resources, Hangzhou 310012, China;
[3] Organic Geochemistry Unit, Key Laboratory of Geoscience Big Data and Deep Resource of Zhejiang Province, School of Earth Sciences, Zhejiang University, Hangzhou 310027, China

**Received 22 May 2024; accepted 20 August 2024; published online 30 September 2024**

**Abstract** Dissolved oxygen (DO) and apparent oxygen utilization (AOU) are essential parameters for evaluating the impact of climate change on marine ecosystems. In this study, we utilized data on DO and AOU collected from the Amundsen Sea (western Antarctic) and the Cosmonaut Sea (eastern Antarctic) during the 38th Chinese National Antarctic Research Expedition, along with chlorophyll *a* (Chl *a*) data, to analyze the impact of primary production and the spatial distribution and structural features of water masses in these regions. The findings show that the standard deviation range of parallel DO samples is between 0.1 and 3.9 μmol·L$^{-1}$, meeting the precision criteria of the survey method. AOU values lower than 0.0 μmol·L$^{-1}$ were commonly observed in the surface waters of both regions, with the highest incidence in the polynya of Amundsen Sea, indicating a strong influence of high primary production. The Cosmonaut Sea exhibited the highest AOU values (higher than 160.0 μmol·L$^{-1}$) in the 75–500 m layer, while AOU value in the Amundsen Sea did not exceed 160.0 μmol·L$^{-1}$, suggesting potential upwelling of Circumpolar Deep Water to 100 m in the Cosmonaut Sea with minimal changes in its properties, whereas significant changes were noted in the properties of upwelling modified Circumpolar Deep Water in the Amundsen Sea. AOU values lower than 125.0 μmol·L$^{-1}$ were detected in the near-bottom waters of the Cosmonaut Sea, indicating the presence of Antarctic Bottom Water.

**Keywords** **dissolved oxygen, apparent oxygen utilization, Southern Ocean, water mass, chlorophyll *a***

**Citation:** Ding Y F, Zhu C F, Zhang C, et al. Distributions of dissolved oxygen and apparent oxygen utilization in the Cosmonaut Sea and Amundsen Sea in austral summer 2022. Adv Polar Sci, 2024, 35(3): 327-369, doi: 10.12429/j.advps.2024.0018

## 1 Introduction

Dissolved oxygen (DO) is crucial for the survival of organisms in marine ecosystems (Gilly et al., 2013). Changes in DO concentration are strongly linked to marine productivity, water mass mixing, temperature, salinity, and organic matter decomposition processes (Böning et al., 2008; Levin, 2018; Matear et al., 2000). The increase of ocean water temperature caused by global warming is expected to result in a continual decline in DO levels (Schmidtko et al., 2017). Studies indicate that by 2100, global oceanic DO levels could decrease by 1%–7%, with this downward trend persisting over an extended period (Keeling et al., 2010; Levin, 2018). Moreover, alterations in ocean circulation may impact DO distribution, potentially leading to enhanced vertical mixing in the Antarctic Bottom

* Corresponding authors. ORCID: 0000-0001-6592-3365. E-mail: jzhao@sio.org.cn (ZHAO Jun). E-mail: jmpan@sio.org.cn (PAN Jianming).

Water (AABW) formation region, facilitating the transport of oxygen-rich surface water to deeper layers (Purkey and Johnson, 2013; Solodoch et al., 2022). Ocean acidification and eutrophication could exacerbate these effects, potentially causing local increases of primary productivity (Schmidtko et al., 2017). This could elevate oxygen consumption during organic matter decomposition processes, resulting in decrease of DO levels in specific water areas. Apparent oxygen utilization (AOU) represents the difference between the theoretical saturated DO and the measured DO concentration, serving as an indirect indicator of organic matter degradation in water bodies. Elevated AOU values typically suggest high biological activity (e.g., organic matter decomposition) and/or longer water residence time. AOU is also a valuable indicator of ocean circulation and mixing, reflecting oxygen consumption from surface to deep water layers (Boyer et al., 1999; Gopinath et al., 2006). Hence, DO and AOU are essential tools for evaluating biogeochemical processes and ecological functions in marine ecosystems. Monitoring these parameters is critical for comprehending the impacts of climate change on marine ecosystems and predicting their future responses.

The Southern Ocean is a crucial region and a sensitive area for global climate change (Park et al., 1998), accounting for 16% of global DO loss, significantly impacting the global distribution of DO (Helm et al., 2011). The Antarctic marginal sea plays a critical role in the formation of global deep ocean currents and exhibits high productivity. Global warming may lead to a reduction in DO in the AABW formation region, linked to changes in glacier melting and precipitation patterns that alter the formation process of Southern Ocean Deep Water and its DO concentration (Schmidtko et al., 2017; Solodoch et al., 2022). Studies have identified local increase processes of oxygen and AOU due to biogeochemical processes and changes in ocean dynamics in the Antarctic marginal sea, related to ocean mixing, upwelling, and seasonal sea ice changes (Arrigo et al., 2008). Surface phytoplankton productivity in this area influences DO distribution across the entire Southern Ocean (Arrigo and van Dijken, 2003; Arrigo et al., 1998). During spring, as sea ice melts, low salinity, iron-rich meltwater is released, forming a lower density freshwater layer conducive to phytoplankton growth (Mendes et al., 2012). In summer, rising sea temperatures and reduced sea ice lead to significant consumption of DO in seawater (Kim and Kim, 2021). Seasonal variations in biological activity can result in notable fluctuations in AOU (McClish and Bushinsky, 2023). Consequently, understanding the complex changes in DO in the Antarctic marginal seas across different seasons and years is essential.

The Amundsen Sea and the Cosmonaut Sea are significant marginal seas in Antarctic. The Amundsen Sea, located in western Antarctic, is experiencing notable warming among the marginal seas of Antarctic (Zhang and Li, 2023). Recent observations show that surface seawater in the Amundsen Sea is warming, while sea ice coverage is decreasing (Stammerjohn et al., 2008). Conversely, the Cosmonaut Sea in eastern Antarctic has been experiencing decreasing temperatures and an expansion of sea ice extent in recent decades (Ludescher et al., 2019). The Amundsen Sea, a deep-water pathway situated on the western side of Antarctic, plays a crucial role in transporting DO from west to east through the Antarctic Circumpolar Current (ACC), which helps to minimize DO differences between various ocean basins (Rintoul and da Silva, 2019). However, the accelerated melting of glaciers in western Antarctic due to global warming is leading to an influx of freshwater into the Amundsen Sea, potentially impacting changes in water density and vertical mixing, which in turn influence DO distribution (Biddle et al., 2017; Wang et al., 2022; Xing et al., 2020). The melting of sea ice and the collapse of ice shelves can alter the water column structure, with water column stability being a critical factor in studying phytoplankton in the region (Mendes et al., 2012). The depth of the mixed layer serves as a key indicator of water column structure, where a shallower mixed layer depth indicates water column stability, and the biomass of phytoplankton (chlorophyll *a* (Chl *a*) concentration) often shows a negative correlation with mixed layer depth in the study area (Hewes et al., 2008). Particularly in summer, the freshwater layer formed by glacier meltwater may impede the downward transport of oxygen-rich surface water, resulting in a reduction in DO supply to the deep-water column (Raiswell et al., 2016; Tagliabue et al., 2009).

Compared to the Amundsen Sea, research on DO in the Cosmonaut Sea is relatively scarce. According to data from the BROKE-West survey, the Cosmonaut Sea is characterized by the widespread presence of year-round ice, strong seasonal variations, and a distinct seasonal mixed layer (Martinson and Iannuzzi, 2013; Meijers et al., 2010). Large polynyas periodically appear in the Cosmonaut Sea (Arbetter et al., 2004). On one hand, these polynyas receive ample sunlight, leading to high primary production (Arrigo et al., 2008). On the other hand, the upwelling in the polynyas, driven by sea surface winds, brings deep-water to the surface, significantly influencing the distribution of DO (Arbetter et al., 2004; Geddes and Moore, 2007). Additionally, the wind fields in the Cosmonaut Sea area cause the large-scale seasonal mixed layer to deepen gradually from west to east (Geddes and Moore, 2007; Park et al., 1998; Williams et al., 2010). Guo et al. (2023) found a correspondence between the AOU values at different depths and water mass characteristics based on DO and AOU data from the 37th Chinese National Antarctic Research Expedition (CHINARE-37). The presence of a narrow continental shelf in the coastal areas of the Cosmonaut Sea hinders the upwelling of Circumpolar Deep Water (CDW) (Guo et al., 2023; Moreau et al., 2023). Overall, there is considerable uncertainty in the understanding of DO and AOU in the Amundsen Sea and Cosmonaut Sea, mainly due to limited geographical

observational data in these regions and the complex influences of factors such as climate warming and glacier melting.

In this study, we utilized DO, AOU, and Chl *a* data obtained during the 38th Chinese National Antarctic Research Expedition (CHINARE-38) in the two seas to analyze the main hydrological characteristics and their variations during the summer. The research aims to provide data support for observing the long-term continuous changes in DO of the Southern Ocean and its impact on the marine ecosystem.

## 2 Materials and methods

### 2.1 Characteristics of water masses, fronts and currents

The Cosmonaut Sea is situated in the western part of Enderby Land in East Antarctica, characterized by complex and variable sea ice conditions (Geddes and Moore, 2007). The Amundsen Sea, a marginal sea located along the coast of Marie Byrd Land in West Antarctica, is positioned between the Ross Sea and the Bellingshausen Sea. For detailed geological information, please refer to Guo et al. (2023). The study area of the Cosmonaut Sea for the CHINARE-38 spans between 30°E–60°E and 62°S–68°S. It can be divided into two regions: the area west of 50°E is predominantly influenced by the Weddell Gyre (Park et al., 2001), while to the east of 50°E, the ACC extends from the north into this region. The study area for the Amundsen Sea of the CHINARE-38 covers the area between 110°W–150°W and 72°S–76°S. Sampling stations from 110°W–120°W encompass the entire polynya. The ACC, Antarctic Slope Current (ASC), Southern Boundary (SB) of ACC, Weddell Gyre (WG), and Ross Gyre (RG) are the primary ocean currents that play pivotal roles in this region (Figure 1).

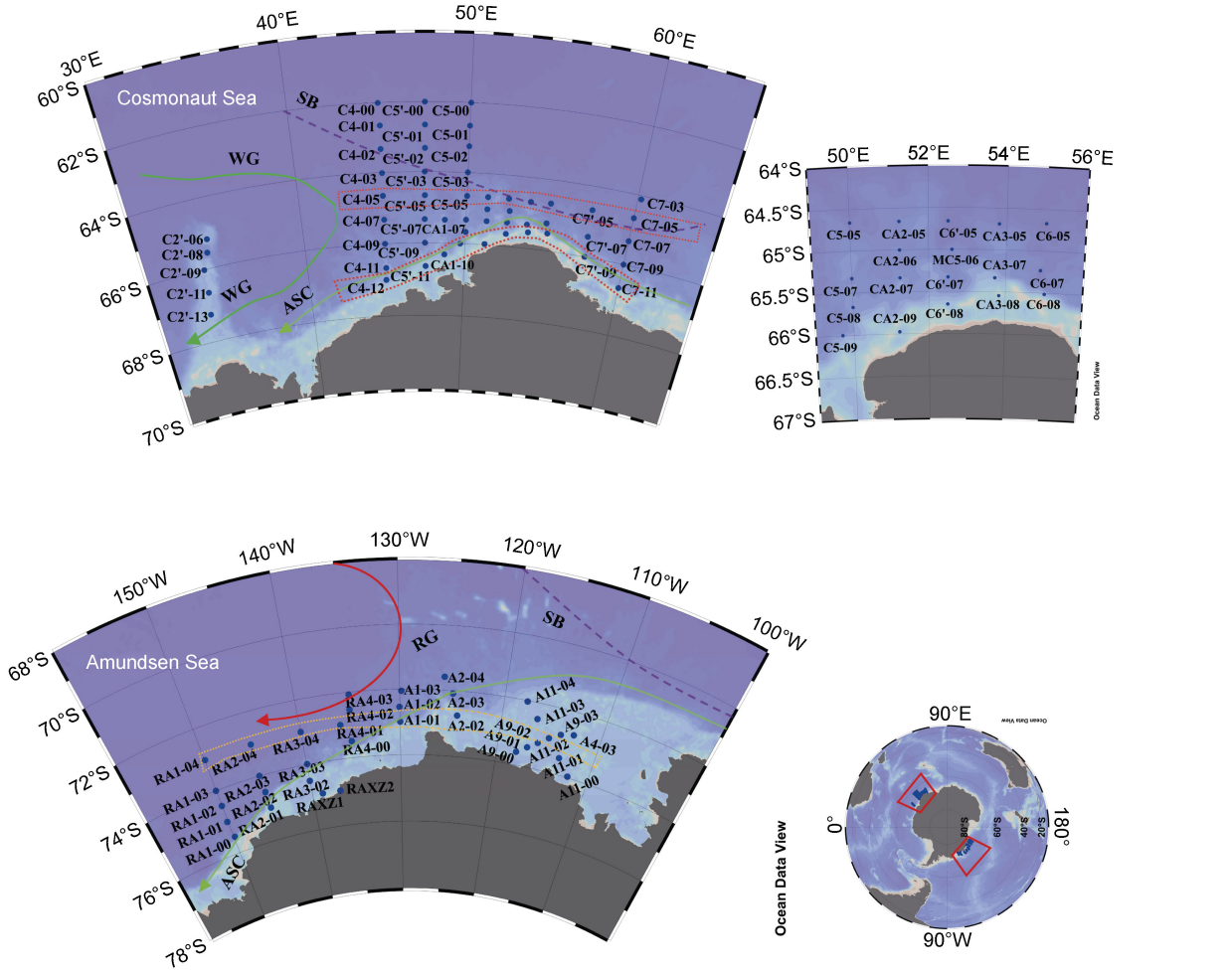


**Figure 1** The sampling stations for DO and Chl *a* in the the Cosmonaut Sea and Amundsen Sea during the summer of 2022 in Antarctic. The primary circulation patterns in the Cosmonaut Sea consist of Southern Boundary of ACC (SB, purple dashed line), Weddell Gyre (WG, green solid line), and Antarctic Slope Current (ASC, yellow-green solid line) (Williams et al., 2010). The red dotted frame marks the positions of two cross-transects, one at 64.6°S and the other near the continental shelf. In the Amundsen Sea, the major circulation patterns comprise the Ross Gyre (RG, red solid line), ASC (yellow-green solid line), and SB (purple dashed line) (Arneborg et al., 2012; Nakayama et al., 2018). The orange dotted frame marks the positions of one cross-transect at 73°S.

### 2.2 Sample collection and determination of DO

The data utilized in this study consist of DO and Chl *a* measurement conducted on-site by the CHINARE-38 in the Cosmonaut Sea and the Amundsen Sea (sampling locations depicted in Figure 1). In the Cosmonaut Sea, comprehensive observations were carried out from 27 January to 26 February, 2022, encompassing a total of 54 sampling sites; whereas in the Amundsen Sea, observations were performed from 24 January to 19 February, 2022, at 34 sampling stations.

Water samples for DO analysis were obtained using a conductivity-temperature-depth (CTD) rosette from standard layers at approximately 2–3 m (logarithmically represented as 5 m), 25 m, 50 m, 75 m, 100 m, 150 m, 200 m, 300 m, 500 m, 1000 m, 2000 m, 3000 m, 4000 m, and the bottom layer, amounting to a total of 66 parallel samples (Table S1). Following collection, the water samples were transferred to brown bottles with a volume of around 120 mL (measured precisely to 0.1 mL). The samples were carefully poured into the bottles through a rubber tube until they filled half the volume of the bottle, ensuring the absence of trapped air bubbles. Subsequently, 1.0 mL of 2.4 mol·L$^{-1}$ $MnCl_2$ solution and 1.0 mL of 1.8 mol·L$^{-1}$ alkaline KI solution (5.4 mol·L$^{-1}$ NaOH) were sequentially added using a calibrated pipette. Upon addition of the reagents, the bottle was promptly sealed and gently inverted. During this process, $O_2$ reacted with manganese ions ($Mn^{2+}$) and hydroxide ions ($OH^-$) to produce a brown precipitate of high-valent manganese ($MnO(OH)_2$), which was utilized for subsequent analysis.

The DO titration was completed within 24 h of sampling using the iodometric titration method outlined in "Part 4: Survey of Chemical Parameters in Sea Water" (GB/T 12763.4—2007) (General Administration of Quality Supervision, Inspection and Quarantine of the People's Republic of China and Standardization Administration of China, 2007). The titration process was carried out using a calibrated Mettler Toledo T5 automatic potentiometric titrator. Once the precipitate settled at the bottom of the brown glass bottle, 1 mL of 1∶3 (V∶V) $H_2SO_4$ was added to dissolve the precipitate and convert iodide ions ($I^-$) to iodine ($I_2$). The content of $I_2$ and the corresponding DO levels were determined through thiosulfate ($Na_2S_2O_3$) titration. The $Na_2S_2O_3$ solution (approximately $1\times10^4$ μmol·L$^{-1}$, calibrated with a $KIO_3$ standard solution) was titrated into the sample using the automatic potentiometric titrator until the endpoint was reached. The DO content was calculated based on the volume of $Na_2S_2O_3$ solution consumed. The standard deviations for seawater standard samples with DO contents <160 μmol·L$^{-1}$ and >550 μmol·L$^{-1}$ should be <±2.8 μmol·L$^{-1}$and <±4.0 μmol·L$^{-1}$, respectively, with an accuracy of DO content determination of 0.6 μmol·L$^{-1}$.

The formula for calculating the concentration of DO (as O atom) is:

$$c(\mathrm{O}) = \frac{V_n \times c}{(V_1 - V_2)\times 2} \tag{1}$$

where, $c$(O) is the concentration (μmol·L$^{-1}$) of DO in seawater samples, $c$ is the calibration concentration (μmol·L$^{-1}$) of $Na_2S_2O_3$ solution, $V_1$ is the volume (mL) of the brown bottle, $V_2$ is the total volume (mL) of $MnCl_2$ and $KIO_3$-NaOH solutions, $V_n$ is the volume (mL) of $Na_2S_2O_3$ solution consumed during titration.

### 2.3 Sample collection and analysis of Chl *a*

Water samples for Chl *a* analysis were collected using a CTD rosette from the surface to a depth of 200 m (0 m, 25 m, 50 m, 75 m, 100 m, 150 m, and 200 m). Following sample collection, the water samples designated for Chl *a* analysis were immediately filtered using a glass fiber filter (Whatman, 0.7 μm, GF/F). Subsequently, extraction was carried out using 90% acetone, and fluorescence measurements were taken using a Turner Designs fluorometer. The specific procedures adhered to the guidelines established by Welschmeyer (1994).

### 2.4 Calculation of AOU

The formula for calculating AOU (as $O_2$ molecule) is:

$$c_{\mathrm{AOU}} = c_{\mathrm{O}}^{\mathrm{S}} - c_{\mathrm{O}} \tag{2}$$

where, $c_{\mathrm{O}}^{\mathrm{S}}$ is the saturation concentration of $O_2$ in the water column at 101.325 kPa atmospheric pressure and 100% humidity, $c_{\mathrm{O}}$ is the concentration of $O_2$ measured on site. AOU<0 indicates that DO is over saturated, and AOU>0 indicates that DO is in a depleted state. $c_{\mathrm{O}}^{\mathrm{S}}$ is related to seawater temperature ($T$) and salinity ($S$), and the calculation formula (see GB/T 12763.4—2007) is:

$$\begin{aligned}\ln c_{\mathrm{O}}^{\mathrm{S}} = \frac{1}{2}\Bigg\{ & -168.938 + 249.6339\left(\frac{100}{T}\right) + 143.3483\ln\left(\frac{100}{T}\right) - \\ & 21.8492\left(\frac{100}{T}\right) + S\left[-0.033096 + 0.014259\left(\frac{100}{T}\right) - \right. \\ & \left. 0.0017\left(\frac{100}{T}\right)^2\right]\Bigg\}\end{aligned} \tag{3}$$

where, $T$ and $S$ were determined and recorded using a pre-calibrated Sea-Bird SBE-9/11 plus CTD system (SeaBird, USA).

### 2.5 Statistical analysis

Data plot and statistical analysis were performed with Ocean Data View software and Origin 9.65 software. Pearson correlation analysis was used between AOU and Chl *a*. The independent *t*-test was used to compare the difference in average values of AOU and Chl *a* in different sea regions. Two-tailed tests of significance were performed using SPSS 25 software (IBM, USA) to identify significant relationships between the measured parameters. The correlations were investigated and considered robust when

$p$<0.05 for the single areas.

# 3 Results

## 3.1 Parallel sample analyses

The range of standard deviation for DO in parallel samples was <0.1–3.9 μmol·L$^{-1}$ (Table S1), which meet the requirements outlined in the investigation standard (GB/T 12763.4–2007). Therefore, the parallelism results meet the requirements for experimental precision. In the Cosmonaut Sea, the range of DO concentration and AOU values were 314.9–790.8 μmol·L$^{-1}$ and −35.3–186.4 μmol·L$^{-1}$, respectively (Table S2). In the Amundsen Sea, the DO concentration and AOU values ranged from 375.6–850.0 μmol·L$^{-1}$ and –56.1–156.5 μmol·L$^{-1}$, respectively (Table S3). Both study areas exhibited well-oxygenated conditions.

## 3.2 Spatial distribution of DO and AOU in the Cosmonaut Sea

The horizontal distribution of DO and AOU in the Cosmonaut Sea was shown in Figure 2 (and Figures S1 and S2). The ranges of DO in the surface, 200 m layer, and bottom layer were 662.1–790.8 μmol·L$^{-1}$ (average (709.0±27.4) μmol·L$^{-1}$), 324.3–672.5 μmol·L$^{-1}$ (average (483.7±106.8) μmol·L$^{-1}$), and 403.7–612.0 μmol·L$^{-1}$ (average (69.3±57.8) μmol·L$^{-1}$), respectively. The corresponding AOU ranges in these layers were −35.3–31.2 μmol·L$^{-1}$ (average (7.6±14.7) μmol·L$^{-1}$), 34.9–181.0 μmol·L$^{-1}$ (average (118.8±40.6) μmol·L$^{-1}$), and 69.3–155.8 μmol·L$^{-1}$ (average (127.8±23.6) μmol·L$^{-1}$). In the surface layer, AOU was <0.0 μmol·L$^{-1}$ in the southwest (C2' transect, stations C4-09 to C4-12, C5-00 to C5-02, and C5'-11). In the 200 m layer, AOU in the north ((163.7±7.1) μmol·L$^{-1}$) (stations C4-00 to C4-03, C4-07 to C4-09, C5'-00 to C5'-03, C5-00, C5-02, CA3-05, C6-05, C7'-05, and C7-03 to C7-07) was significantly ($p$<0.01) higher than that in the south ((96.3±30.2) μmol·L$^{-1}$). Given that most of the sampling depths in the CHINARE-38 only reached around 1000 m, only on the C4 transect are there 6 stations, on the C5 transect 1 station, and on the C7 transect 1 station where sampling depth reaches the bottom. In the bottom layer, the value of AOU was less than 130.0 μmol·L$^{-1}$ at stations C4-00 to C4-02 and stations C4-07 to C4-09.

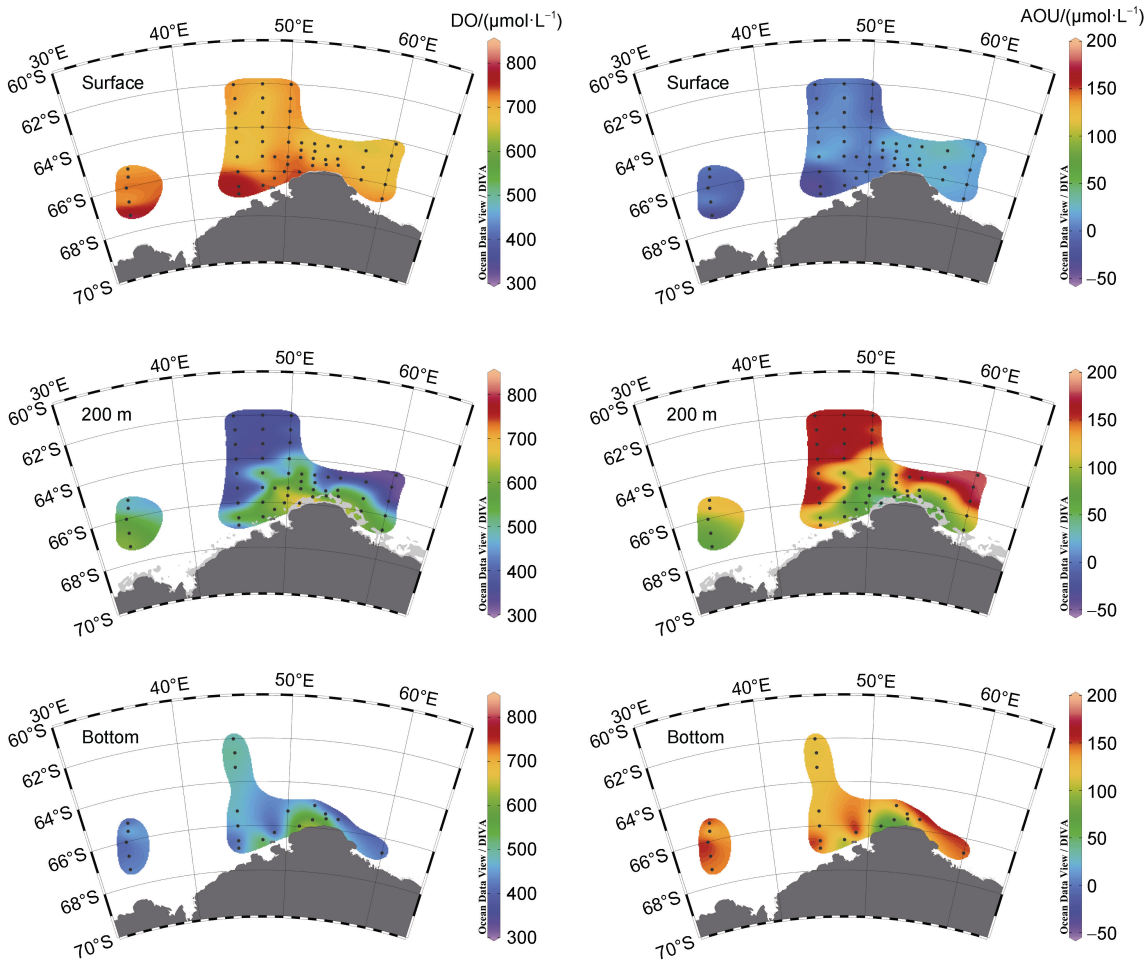


**Figure 2** Horizontal distributions of DO and AOU in the surface layer, 200 m layer and bottom layer of the Cosmonaut Sea.

The vertical distribution of DO and AOU in the C2', C4, C5, C7, 64.6°S, and coastal transects of the Cosmonaut Sea was shown in Figure 3. Across all transects, the DO concentration in the euphotic zone declined rapidly with increasing water depth, reaching a minimum between 200 and 1000 m before slightly increasing. At the surface and at a depth of 25 m, AOU remained consistently below 30.0 μmol·L$^{-1}$. In the C4 and C5 transects, AOU increased gradually with depth in high-latitude coastal areas, while it rose rapidly in low-latitude open sea areas between 50 and

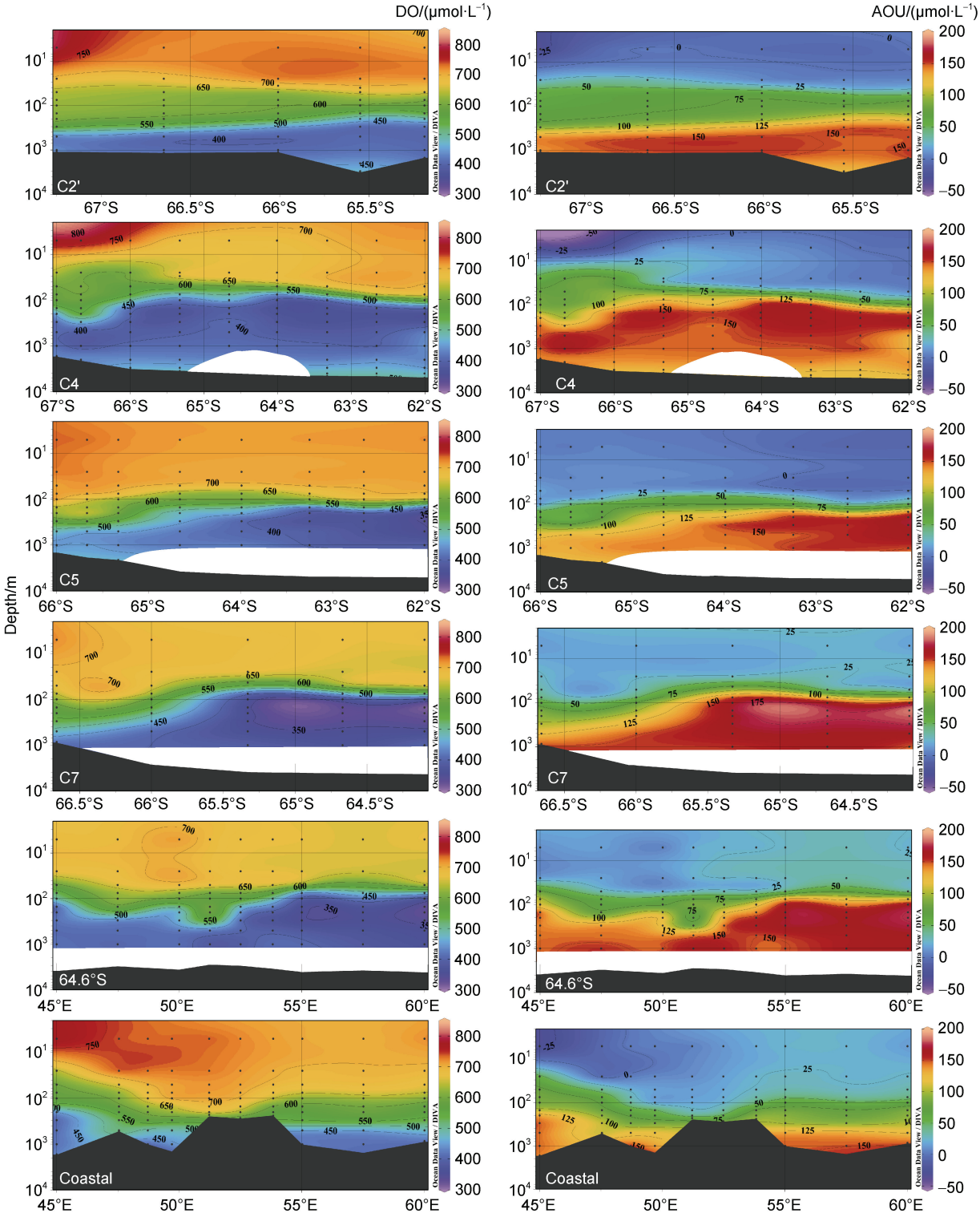


**Figure 3** Vertical distributions of DO and AOU along transects C2', C4, C5, C7, 64.6°S and coastal transects in the Cosmonaut Sea. Note: depth was displayed in logarithmic form.

300 m. A comparison with the 64.6°S transects indicated that the surface AOU in coastal transects is below 0.0 μmol·L$^{-1}$. Additionally, compared to the 64.6°S transect, the AOU in coastal transects, with depths ranging from 100 to 1000 m, was notably lower.

### 3.3 Spatial distribution of DO and AOU in the Amundsen Sea

The spatial distribution of DO and AOU in the Amundsen Sea was shown in Figure 4 and Figures S3–S4. The concentration ranges of DO in the surface, 200 m layer, and bottom layer were as follows: 721.3–850.0 μmol·L$^{-1}$ (average (776.3±34.7) μmol·L$^{-1}$), (406.9–719.7) μmol·L$^{-1}$ (average (550.1±74.6) μmol·L$^{-1}$), and (405.0–634.4) μmol·L$^{-1}$ (average (451.3±40.4) μmol·L$^{-1}$), respectively. The corresponding AOU ranged at these depths are as follows: −56.1–13.4 μmol·L$^{-1}$ (average (−18.2±20.0) μmol·L$^{-1}$), 12.0–146.7 μmol·L$^{-1}$ (average (95.8±28.7) μmol·L$^{-1}$), and 57.8–149.7 μmol·L$^{-1}$ (average (131.2±15.5) μmol·L$^{-1}$). Regarding the spatial distribution, in the surface layer, AOU>0.0 μmol·L$^{-1}$ was only observed on the west side (stations RA1-01 to RA1-03, RA2-02 to RA2-04, and RA4-02 to RA4-03). However, in the 200 m layer, the AOU in the deep-sea regions (stations RA1-04, RA2-04, RA3-04, RA4, and A1 transect) ((130.3±14.8) μmol·L$^{-1}$) was higher than that in the coastal regions ((81.5±19.1) μmol·L$^{-1}$). There were no significant differences in the horizontal distribution of DO and AOU in the bottom layer.

The vertical distribution of DO and AOU along transects RA1, RA3, A11, A9, and 73°S in the Amundsen Sea was shown in Figure 5. In the euphotic zone, DO concentration decreased greatly with depth, reaching a minimum between 200 and 1000 m. Subsequently, DO slightly increased with depth, while AOU exhibited the opposite trend. On the RA1 and RA3 transects, AOU increased from <30.0 μmol·L$^{-1}$ at the surface and 25 m depth to over 150.0 μmol·L$^{-1}$ between 200 and 500 m, then gradually decreased to 130.0 μmol·L$^{-1}$ at depths exceeding 3000 m. The distribution of DO and AOU on the RA1 transect demonstrated a consistent trend from nearshore to offshore areas, with no significant latitude differences. AOU in the euphotic zone on the A11 and A9 transects ((32.8±54.9) μmol·L$^{-1}$) was significantly lower ($p$<0.01) than that on other transects ((54.5±49.7) μmol·L$^{-1}$). Compared to

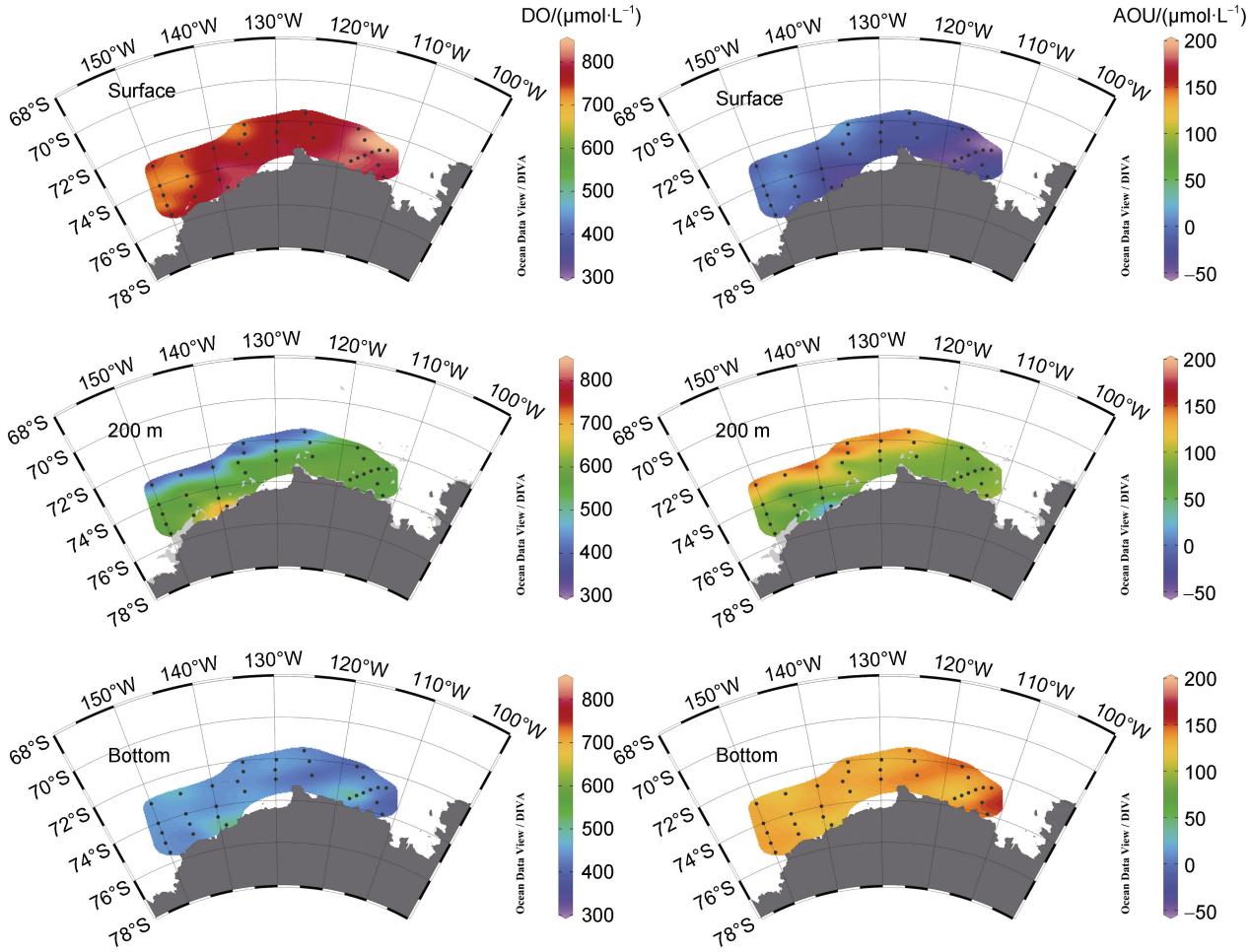


**Figure 4** Horizontal distributions of DO and AOU in the surface layer, 200 m layer and bottom layer of the Amundsen Sea.

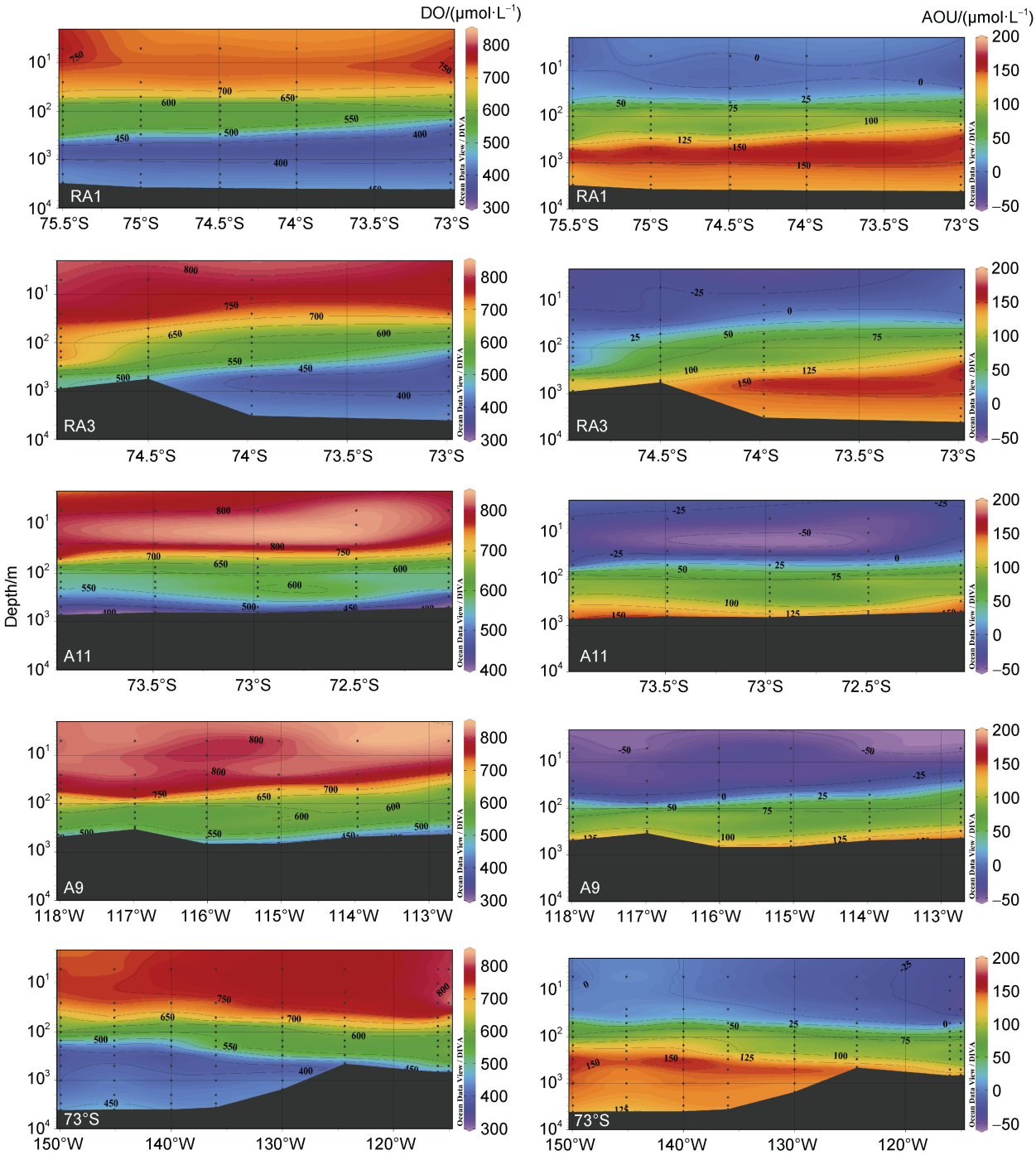


**Figure 5** Vertical distributions of DO and AOU along transects RA1, RA3, A11, A9 and 73°S in the Amundsen Sea. Note: depth was displayed in logarithmic form.

non-polynya regions of the Amundsen Sea and the Cosmonaut Sea, the A11 and A9 transects exhibited low AOU (<0.0 μmol·L$^{-1}$) down to 75 m depth, likely due to the presence of polynya in the Amundsen Sea. Furthermore, significant differences between the eastern and western parts were observed along the 73°S transect. In the western part, AOU exceeded 150.0 μmol·L$^{-1}$ at 300 m depth for stations RA1-04 and RA3-04, while in the eastern part, stations A9-02 and A11-02 showed AOU of approximately 85.0 μmol·L$^{-1}$ at the same depth.

### 3.4 Spatial distribution of Chl *a* in the Cosmonaut Sea and the Amundsen Sea

The horizontal distribution of Chl *a* in the Cosmonaut Sea was shown in Figure 6. The concentrations of Chl *a* in the surface and 200 m layers range from 0.02 to

1.22 mg·m$^{-3}$ (average (0.46±0.34) mg·m$^{-3}$) and from 0.00 to 0.61 mg·m$^{-3}$ (average (0.04 ±0.10) mg·m$^{-3}$), respectively. Elevated Chl *a* values (>0.65 mg·m$^{-3}$) were observed in the surface layer at stations C2'-13, C4-11 to C4-12, and C5'-11 on the southwest side, with corresponding AOU values all below 0.0 μmol·L$^{-1}$. In the 0–100 m layer, Chl *a* concentrations near the continental shelf stations were significantly higher ($p$<0.05) compared to those in the northern region. Conversely, in the 200 m layer, Chl *a* exhibited a uniform spatial distribution.

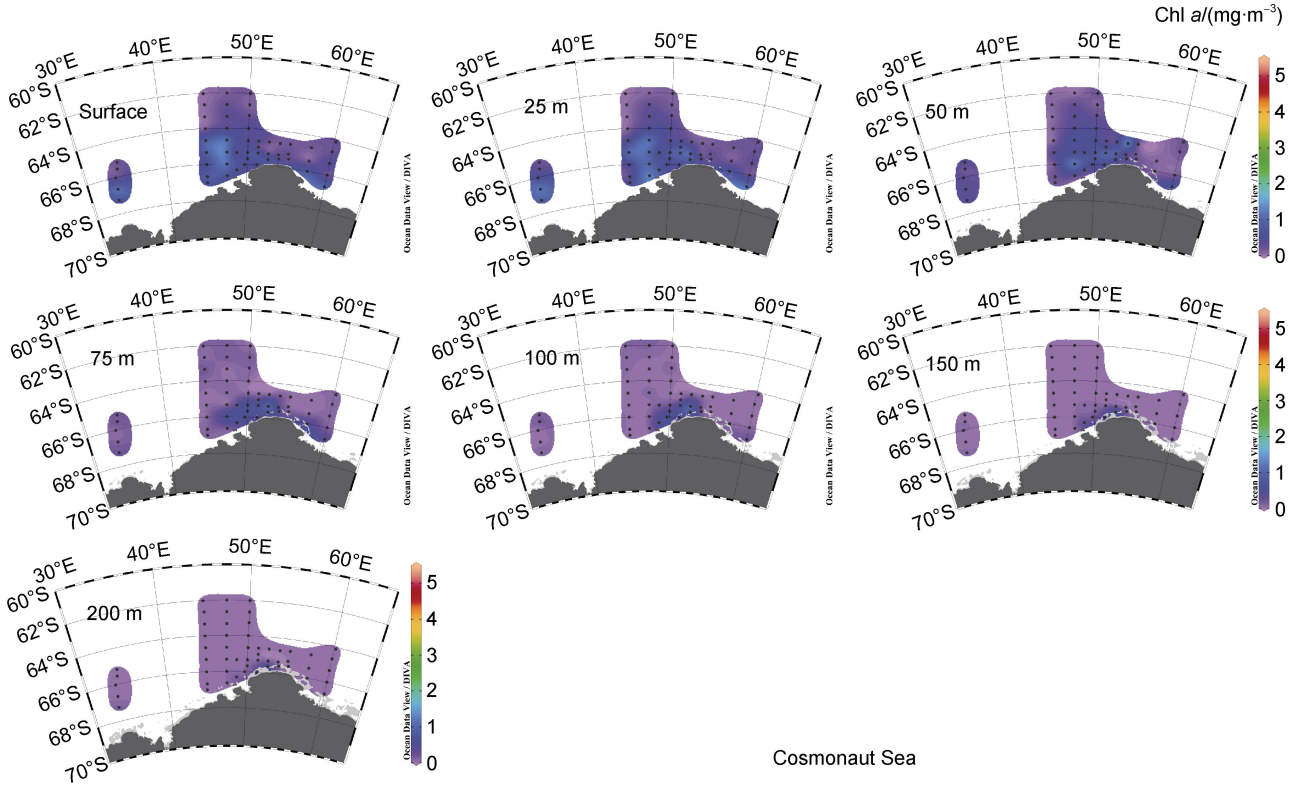


**Figure 6** Horizontal distributions of Chl *a* in the Cosmonaut Sea (units: mg·m$^{-3}$).

The horizontal distribution of Chl *a* in the Amundsen Sea was shown in Figure 7. The Chl *a* range in the surface and 200 m layers were 0.78–5.16 mg·m$^{-3}$ (average (2.34±1.16) mg·m$^{-3}$) and 0.06–0.53 mg·m$^{-3}$ (average (0.21±0.14) mg·m$^{-3}$), respectively. In the surface layer, transects A11 and A9, as well as stations RAXZ1 and RAXZ2, had Chl *a* levels >1.40 mg·m$^{-3}$, with corresponding AOU values <−25.0 μmol·L$^{-1}$. The high Chl *a* (>1.40 mg·m$^{-3}$) in transects A11 and A9 can extend to depths of up to 75 m. In the 200 m layer, the horizontal distribution of Chl *a* also did not show a clear spatial trend.

# 4 Discussion

## 4.1 The AOU indication of water masses

AOU serves as a reflection of the redox state of water masses, making it a crucial parameter in water mass analysis. It also has significant implications to reveal the vertical distribution and stratification of water mass (Iida et al., 2013). Combined with other physicochemical parameters, AOU can help identify specific water mass types (Zhang et al., 2024). In this study, we examined the vertical AOU profiles in the Amundsen Sea and the Cosmonaut Sea in February 2022 (Figure 8). By utilizing potential temperature ($\theta$) and salinity data collected during the CHINARE-38 and referencing previous studies by Kim and Lee (2005), Kim et al. (2016), Meijers et al. (2010), and Williams et al. (2010), we were able to distinguish various water masses in these regions, including Summer Surface Water (SSW), Winter Remnant Shelf Water (WRSW), CDW, modified Circumpolar Deep Water (mCDW), Warm Deep Water (WDW), and AABW. Additionally, we identified fronts such as SB of the ACC, Antarctic Slope Front (ASF), and Southern Antarctic Circumpolar Current Front (sACCf) (Figures S5 and S6).

Based on the vertical potential temperature and salinity profiles (Figures S5 and S6) in conjunction with AOU, the Amundsen Sea displayed three distinct water masses: SSW, WRSW, and mCDW (Figure 8b). The Amundsen Sea SSW exhibits a broad temperature range (–1.5 ℃<$\theta$<2.0 ℃), low salinity ($S$<34.2), and AOU<0.0 μmol·L$^{-1}$, primarily influenced by processes such as summer ice melt and solar radiation. Increased surface radiation leads to higher SSW temperatures, low summer wind speeds, and shallow mixing depths (Westwood et al., 2010; Zhang et al., 2022).

In the Amundsen Sea Polynya (ASP) region, $S$<33.7, and AOU<–25.0 μmol·L$^{-1}$. WRSW is situated beneath the shallow layer of SSW, maintaining the thermohaline characteristics of the winter water mass, with $\theta$<–1.5 ℃, 34.2<$S$<34.5, and 0.0 μmol·L$^{-1}$<AOU<100.0 μmol·L$^{-1}$. WRSW is observed at depths of 30–50 m in the RA1 and RA3 transects, while in the A11 and A9 transects, WRSW begins at depths of 60–80 m.

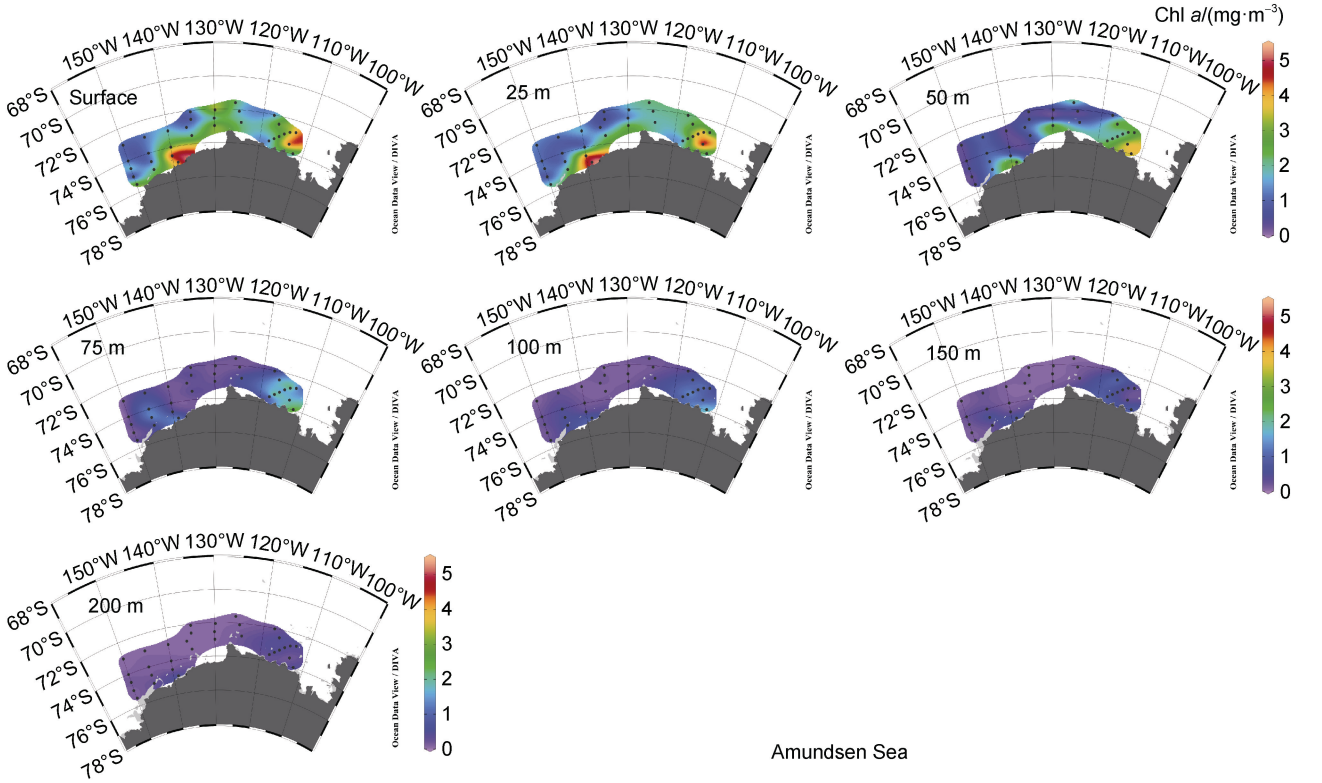


**Figure 7** Horizontal distributions of Chl *a* in the Amundsen Sea (units: mg·m$^{-3}$).

In the surface water layer (0–25 m), the negative AOU values in transects A11 and A9 exhibited a significantly wider depth range compared to transects RA1 and RA3. This difference is attributed to the presence of a thicker SSW. The higher water temperature in the SSW enhances phytoplankton growth, thereby increasing DO levels in the SSW. Furthermore, there is a more pronounced gas exchange between the SSW and the atmosphere, leading to an increased influx of DO and subsequently lowering the AOU values (An et al., 2012). At depths ranging from 150–500 m, the Amundsen Sea continental shelf area (transects RA1 and RA3) displayed AOU values exceeding 150.0 μmol·L$^{-1}$, with the potential for CDW ($\theta$>1.5 ℃) from RA3 flowing southward towards approximately 74°S. Concurrently, observations along the 73°S transect reveal elevated AOU values (>150.0 μmol·L$^{-1}$) west of 130°W (Figure 5), indicating characteristics of CDW upwelling. This phenomenon is closely linked to the incursion of warm mCDW in the Amundsen Sea continental shelf region. Previous studies have demonstrated that CDW penetrates through the troughs (Jacobs et al., 2012). The intrusion of warm mCDW into the Amundsen Sea continental shelf region triggers basal ice shelf melting, which is a critical area for West Antarctic Ice Sheet melting (Drijfhout et al., 2024). Additionally, research has shown that mCDW transports more heat into the ASP, leading to a vertical convergence of water properties and the formation and accumulation of high-density shelf water (Cheng et al., 2022).

This study integrates AOU with water masses and reveals that the Cosmonaut Sea prominently displayed four water masses (Figure 8a). In the surface Cosmonaut Sea, two water mass (SSW and WRSW) characteristics are evident. Notably, at depths of 25–50 m, the AOU corresponding to WRSW is significantly more positive compared to that in the Amundsen Sea. In contrast, at depths of 75–300 m, the AOU values corresponding to WRSW in both sea areas are quite similar, ranging from 50 to 100 μmol·L$^{-1}$. In the upper to middle layers of the open sea in the low-latitude region of the Cosmonaut Sea, CDW ($\theta$>–1.5 ℃) can upwell southward to around 64°S (western transect C4) and even 65.3°S (eastern transect C7) at a depth of 100 m without alteration, with AOU>160.0 μmol·L$^{-1}$ during this process. Transects C5 and C7 demonstrate that mCDW continues to intrude into high-latitude areas, correlating with a decreasing trend in AOU. In the continental shelf coastal region, mCDW penetrates beneath the ice shelf edge, generating colder and fresher water masses, ultimately leading to the formation of Antarctic Surface Water through meridional overturning, bringing

substantial nutrients to the surface waters (Williams et al., 2010). Conversely, in the western transects of the Cosmonaut Sea, transects C2' and C4 are influenced by WDW rich in nutrients induced by the WG near 65.5°S. WDW has potential temperatures above 0.6 ℃ (Figure S5), with a relatively high AOU exceeding 150.0 μmol·L$^{-1}$ (Figure 3). This upwelling flow of WDW continuously transports trace elements such as iron upward to the euphotic zone (Moreau et al., 2023). Thus, AOU serves as an indicator that upwelling transports nutrients from deep waters to the euphotic zone.

In the deep-sea region with depths exceeding 3000 m, the presence of AABW was observed in the Cosmonaut Sea. During CHINARE-38, most observation stations were limited to depths over 1000 m, and the minimum depth at which AABW was observed was around 3500 m. This water mass originates from the adjacent area of Darnley Corner Bottom Water, with its temperature gradually decreasing with depth (Kitade et al., 2014; Li et al., 2024). Increased sea ice production in the Darnley Corner Polynya leads to the formation of AABW, which then flows westward (Tamura et al., 2008). The AOU in this area can be as low as <125.0 μmol·L$^{-1}$, suggesting the presence of AABW (with $\theta$<0.0 ℃) (Figures 8 and S6). Within the AABW water mass, AOU decreases with depth, consistent with the gradual increase in DO observed in the western part of the Darnley Corner Polynya between 3200 and 3800 m (Gao et al., 2022).

On the whole, AOU at different depths is influenced by the water mass, along with oceanographic parameters such as potential temperature and salinity, it can provide insights into the characteristics and variations of the water mass.

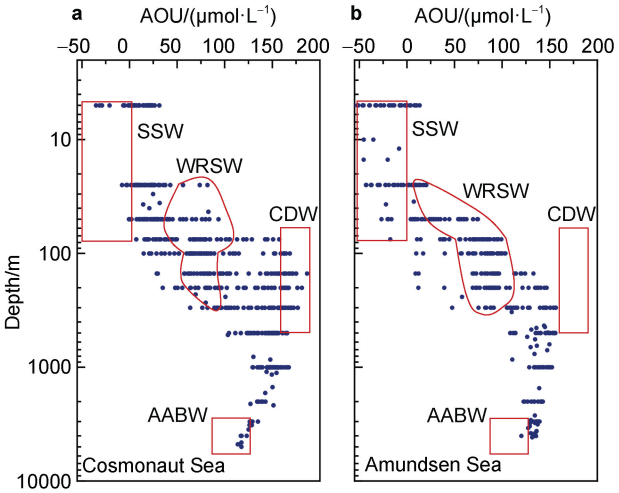


**Figure 8** Profile view of AOU of the Cosmonaut Sea (**a**) and Amundsen Sea (**b**) in February 2022.

## 4.2 Impact of primary production on the spatial distribution of surface AOU

The concentration of DO in the upper layer of the ocean is influenced by factors such as the solubility of oxygen in seawater, biological activities (such as microbial decomposition of organic matter), and the contribution from primary production. A positive AOU value indicates a dominant role of microbial decomposition, while a negative AOU value suggests a greater impact of photosynthesis, which is part of the primary production process (Kostyleva et al., 2022). This research investigated the connection between surface Chl *a* and AOU (Figure 9a). The results revealed a significant negative correlation between surface AOU and Chl *a* within the study area ($p$<0.01, $r$=−0.71, $n$=87), indicating a consistent influence of Chl *a* on surface AOU during both summer seasons in the two regions.

The relationship between AOU and Chl *a* in the entire study area can be categorized into three scenarios. The first dataset (green dots in Figure 9a) pertained to stations located west of 120°W in the Amundsen Sea, where AOU and surface Chl *a* exhibited a negative correlation, indicating a decline in AOU values with increasing Chl *a* concentration. This underscored notable spatial variations in AOU and Chl *a* level in the western sector of the Amundsen Sea. The second dataset (yellow triangles) in Figure 9a was situated in the ASP region, showing negative AOU values and elevated Chl *a* concentration. The weak linear association between Chl *a* and AOU implied a more uniform nature of both parameters within polynyas. The negative AOU values were likely attributable to the intensity of phytoplankton photosynthesis. Previous research has demonstrated a positive relationship between Chl *a* and DO in the ASP, linked to phytoplankton primary productivity (Hu et al., 2023). Arrigo et al. (2008) identified the ASP as one of the 37 coastal polynyas in the Southern Ocean with the highest primary productivity. Phytoplankton biomass in the ASP region surpasses that in ice-covered areas (Lee et al., 2012). The elevated Chl *a* level in coastal polynyas in the Southern Ocean may be attributed to increased iron input into surface waters, which stimulates phytoplankton growth (Arrigo et al., 2015). Additionally, prior studies in the Ross Sea polynya (Arrigo et al., 2000) and ASP (Alderkamp et al., 2012) have indicated a negative correlation between Chl *a* and mixed layer depth, ascribed to better light conditions in warmer and shallower mixed layers rather than enhanced phytoplankton growth activity (Arrigo et al., 2015). This indicates that the AOU in the Amundsen Sea is primarily related to photosynthesis.

The third dataset, represented by blue cubes, pertains to the station points in the Cosmonaut Sea during February of summer. This dataset was characterized by Chl *a* concentrations all lower than 1.30 mg·m$^{-3}$, with a narrow range of variation, while the AOU ranges from –35.3 to 31.2 μmol·L$^{-1}$. The correlation between AOU and Chl *a* content was not statistically significant ($p$>0.05, $r$=−0.16, $n$=53), suggesting that AOU in the Cosmonaut Sea is influenced by factors other than Chl *a*. Previous studies have shown that in the northeastern Black Sea, the lack of correlation between summer AOU and Chl *a* is attributed to

the extensive phytoplankton bloom in spring, resulting in the accumulation of semi-stable organic matter that degrades in summer, thus limiting phytoplankton primary production (Cauwet et al., 2002; Kostyleva et al., 2022). This finding aligns with observations by Nielsen et al. (2023), who noted that due to significant nitrogen consumption, phytoplankton growth in late summer in the Bering Strait is generally constrained (Nielsen et al., 2023). These results suggest the existence of other influencing factors on AOU that warrant further investigation.

Furthermore, this study examined the relationship between surface AOU and Chl *a* levels in various regions of the Antarctic marginal seas (Figure 9b). The results showed that there was a negative correlation between AOU and Chl *a* for the whole dataset, suggesting that surface AOU is primarily controlled by primary production. However, significant variations are observed among different regions. For the open ocean areas, it is characterized by positive AOU (i.e., AOU>0.0 μmol·L$^{-1}$) and minimal Chl *a* concentrations, indicating a prevalence of microbial consumption over primary production in these regions. For the coastal areas, it is characterized by negative AOU (i.e., AOU<0.0 μmol·L$^{-1}$) and higher Chl *a* concentrations, indicating that primary production is dominant. Especially, for the polynya regions, it is characterized by more negative AOU (i.e., AOU<–30.0 μmol·L$^{-1}$) and much higher Chl *a* concentrations, where the primary productivity are significantly higher than other coastal areas. We also noted that in certain regions and certain time, such as February in southwest Cosmonaut Sea and ice shelf front of Prydz Bay, it was characterized by negative AOU and very low Chl *a* concentrations. We will discuss this phenomenon in the next section.

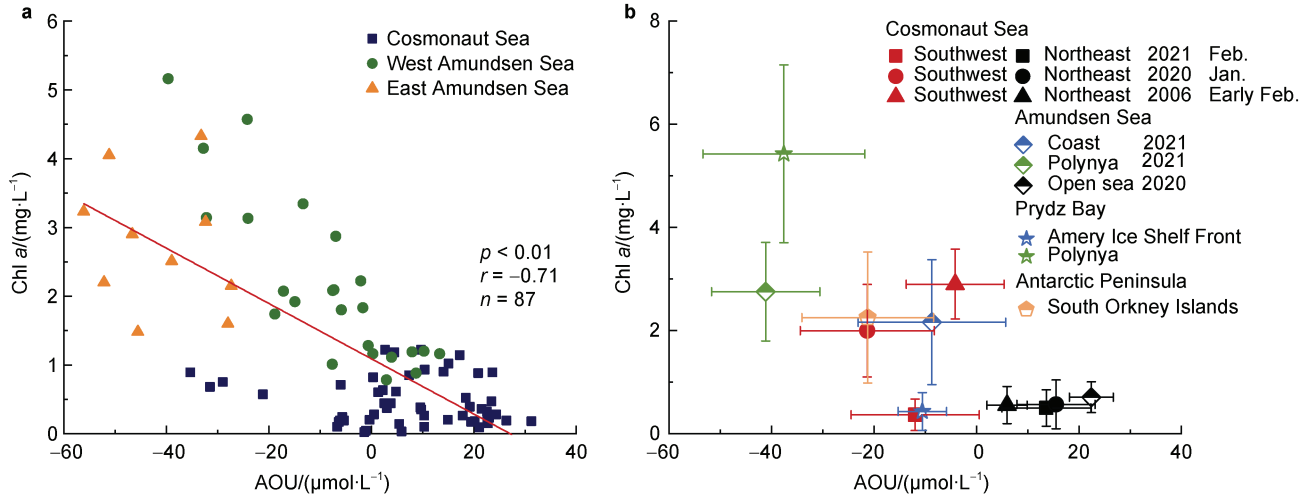


**Figure 9** **a**, correlation analysis between Chl *a* and AOU in surface layer of the Cosmonaut Sea and Amundsen Sea; **b**, analysis of AOU and Chl *a* concentrations at the surface (0 m) in various regions of the Southern Ocean. Error bars indicate the standard deviation of the data. Data from 2006 were collected during the BROKE-West expedition, data from 2020 were from CHINARE-37, and data from 2021 were from CHINARE-38. Data from Prydz Bay were obtained from Han et al. (2019), while data from the northern tip of the Antarctic Peninsula were sourced from Feng et al. (2022). The category "coast" pertains to data that excludes specific areas.

### 4.3 Intermonthly variability of AOU in the Cosmonaut Sea

AOU in the extremely shallow layer is influenced by many factors, such as sea ice melting, solar irradiance and wind mixing. These factors affect the changes in AOU by influencing phytoplankton growth. Primary production was found to be directly related to DO supply, with significant differences in summer months (Hewes et al., 2008).

The Cosmonaut Sea dataset includes comprehensive data from three expeditions, allowing us to analyze the variations in the Cosmonaut Sea specifically during the austral summer months of January and February. The majority of the CHINARE-38 was conducted in February 2022 in the Cosmonaut Sea, which was one month later than CHINARE-37. These two years were at different stages of sea ice retreat. CHINARE-37 took place during the early stage of sea ice melting, while CHINARE-38 was in the late stage, with minimal sea ice distribution north of 66°S and scattered sea ice in the nearshore areas (Li et al., 2024). During the CHINARE-38, it was observed that the surface waters of the Cosmonaut Sea were warmer in summer compared to CHINARE-37, particularly at the nearshore area of transect C4 (i.e., stations C4-09 to C4-12) (Figure S6), and the AOU was <0.0 μmol·L$^{-1}$, attributing to higher primary productivity associated with local sea ice coverage and the inflow of meltwater (Park et al., 1998). Although a similar range of AOU in the southwest Cosmonaut Sea during the three expeditions, the Chl *a* concentrations were significantly lower in February 2022 (Figure 9b). After the flourishing of phytoplankton in summer, zooplankton will come to feed, and this process takes some time to develop (Mou et al., 2021; Swadling et al., 2010). Therefore, low levels of Chl *a* were observed in February, mainly attributed to predation by zooplankton rather than low primary productivity. The situation of low

Chl *a* was also observed at the ice shelf front of Prydz Bay (Yang et al., 2011) (Figure 9b). Notably, the AOU values for February 2022 (CHINARE-38) and February 2006 (BROKE-West) were comparable, but the Chl *a* was significantly higher in the latter than in the former. This indicates that there are significant interannual differences in the grazing of phytoplankton by zooplankton, possibly due to the strong interannual variations in environmental factors in the Southern Ocean (Pinkerton et al., 2020). Therefore, more interdisciplinary field investigations and research are needed to gain a deeper understanding of the impact of environmental changes on ecosystems.

Additionally, we observed that the surface levels of AOU and Chl *a* showed consistent patterns across the three years in the northeastern region of the Cosmonaut Sea (AOU>0.0 μmol·L$^{-1}$, Chl *a*<1.00 mg·m$^{-3}$, Figure 9b). This indicates that there are no significant intermonthly differences in the surface waters of the open ocean. The cross-transect at 64.6°S (Figure 3) indicated that the CDW extended to 64°S in transect C4, while in transect C7, the CDW reached up to 65.3°S, showing a clear trend of southward intrusion of the CDW. The upwelling depth of warm CDW in February was around 100 m, which is shallower than in January. This was very likely because our AOU values in the surface layer in February were located closer to the high-latitude continental shelf. Furthermore, there were no significant differences in the AOU of bottom waters between three expeditions, indicating a stable structure of the AABW with minimal monthly variations.

# 5 Summary

This study analyzed the spatial distribution characteristics of DO and AOU in the Amundsen Sea and the Cosmonaut Sea during austral summer, using data collected from CHINARE. The results indicated that in surface waters with AOU>0.0 μmol·L$^{-1}$, biological consumption was the prevailing factor. While for AOU<0.0 μmol·L$^{-1}$, primary production was the dominant factor, particularly evident in the values of ASP, highlighting the substantial impact of high primary productivity. A summary of multi-year data revealed that there are no significant seasonal differences in AOU in the Cosmonaut Sea. The highest AOU values (>160.0 μmol·L$^{-1}$) in the 100–300 m layer were observed in the Cosmonaut Sea, suggesting that CDW upwells to at least 100 m with minimal changes in properties. Conversely, the AOU in the Amundsen Sea did not exceed 160.0 μmol·L$^{-1}$, indicating notable changes in properties during the CDW intrusion process. Furthermore, AOU value less than 125.0 μmol·L$^{-1}$ was detected in bottom waters of the Cosmonaut Sea, indicating the presence of AABW. Long-term monitoring of DO and AOU is essential to further validate our findings.

**Acknowledgments** The authors wish to thank the CHINARE-38 team members and the crew of R/V *Xuelong* and R/V *Xuelong 2* for helping collect water samples and temperature and salinity data. Special thanks are extended to researchers He Shichang and Zhang Naixing for their contributions to the collection and determination of dissolved oxygen in the Amundsen Sea. The study was financially supported by the Scientific Research Fund of the Second Institute of Oceanography, MNR (Grant nos. JG2211 and JG2212), the National Polar Special Program "Impact and Response of Antarctic Seas to Climate Change" (Grant nos. IRASCC 01-01-02A and IRASCC 02-02), the National Key Research and Development Program of China (Grant no. 2022YFE0136500) and the National Natural Science Foundation of China (Grant no. 41976228). We would like to thank the anonymous reviewers and Associate Editor Dr. Zhan Liyang for their helpful remarks.

## References

Alderkamp A C, Mills M M, van Dijken G L, et al. 2012. Iron from melting glaciers fuels phytoplankton blooms in the Amundsen Sea (Southern Ocean): Phytoplankton characteristics and productivity. Deep Sea Res Part II Top Stud Oceanogr, 71: 32-48, doi:10.1016/j.dsr2.2012.03.005.

An Y Z, Zhang R, Wang H Z, et al. 2012. Study on calculation and spatio-temporal variations of global ocean mixed layer depth. Chin J Geophys, 55(7): 2249-2258, doi:10.6038/j.issn.0001-5733.2012.07.011 (in Chinese with English abstract).

Arbetter T E, Lynch A H, Bailey D A. 2004. Relationship between synoptic forcing and polynya formation in the Cosmonaut Sea: 1. Polynya climatology. J Geophys Res, 109(C4): C04022, doi:10.1029/2003jc001837.

Arneborg L, Wåhlin A K, Björk G, et al. 2012. Persistent inflow of warm water onto the central Amundsen shelf. Nat Geosci, 5: 876-880, doi:10.1038/ngeo1644.

Arrigo K R, van Dijken G L. 2003. Phytoplankton dynamics within 37 Antarctic coastal polynya systems. J Geophys Res Oceans, 108(C8): 3271, doi:10.1029/2002jc001739.

Arrigo K R, Worthen D, Schnell A, et al. 1998. Primary production in Southern Ocean waters. J Geophys Res Oceans, 103(C8): 15587-15600, doi:10.1029/98jc00930.

Arrigo K R, DiTullio G R, Dunbar R B, et al. 2000. Phytoplankton taxonomic variability in nutrient utilization and primary production in the Ross Sea. J Geophys Res Oceans, 105(C4): 8827-8846, doi:10.1029/1998jc000289.

Arrigo K R, van Dijken G, Long M. 2008. Coastal Southern Ocean: a strong anthropogenic $CO_2$ sink. Geophys Res Lett, 35(21): L21602, doi:10.1029/2008gl035624.

Arrigo K R, van Dijken G L, Strong A L. 2015. Environmental controls of marine productivity hot spots around Antarctica. J Geophys Res Oceans, 120(8): 5545-5565, doi:10.1002/2015jc010888.

Biddle L C, Heywood K J, Kaiser J, et al. 2017. Glacial meltwater identification in the Amundsen Sea. J Phys Oceanogr, 47(4): 933-954, doi:10.1175/jpo-d-16-0221.1.

Böning C W, Dispert A, Visbeck M, et al. 2008. The response of the Antarctic Circumpolar Current to recent climate change. Nat Geosci, 1: 864-869, doi:10.1038/ngeo362.

Boyer T, Conkright M E, Levitus S. 1999. Seasonal variability of dissolved oxygen, percent oxygen saturation, and apparent oxygen utilization in the Atlantic and Pacific Oceans. Deep Sea Res Part I Oceanogr Res Pap, 46(9): 1593-1613, doi:10.1016/s0967-0637(99)00021-7.

Cauwet G, Déliat G, Krastev A, et al. 2002. Seasonal DOC accumulation in the Black Sea: a regional explanation for a general mechanism. Mar Chem, 79(3/4): 193-205, doi:10.1016/S0304-4203(02)00064-6.

Cheng L Q, Ye W J, Zhang C L, et al. 2022. Evolution of water structure under the influence of mCDW intrusion on the continental shelf of Vincennes Bay, Antarctica. Chin J Polar Res, 34(1): 51-61, doi:10.13679/j.jdyj.20210014 (in Chinese with English abstract).

Drijfhout S S, Bull C Y S, Hewitt H, et al. 2024. An Amundsen Sea source of decadal temperature changes on the Antarctic continental shelf. Ocean Dyn, 74(1): 37-52, doi:10.1007/s10236-023-01587-3.

Feng Y B, Li D, Zhao J, et al. 2022. Environmental drivers of phytoplankton crops and taxonomic composition in northeastern Antarctic Peninsula adjacent sea area. Acta Oceanol Sin, 41(1): 99-117, doi:10.1007/s13131-021-1865-4.

Gao L B, Zu Y C, Guo G J, et al. 2022. Recent changes and distribution of the newly-formed Cape Darnley Bottom Water, East Antarctica. Deep Sea Res Part II Top Stud Oceanogr, 201: 105119, doi:10.1016/j.dsr2.2022.105119.

Geddes J A, Moore G W K. 2007. A climatology of sea ice embayments in the Cosmonaut Sea, Antarctica. Geophys Res Lett, 34(2): L02505, doi:10.1029/2006gl027910.

General Administration of Quality Supervision, Inspection and Quarantine of the People's Republic of China and Standardization Administration of China. 2007. Specifications for the oceanographic survey – Part 4: Survey of chemical parameters in sea water: GB/T 12763.4—2007. Beijing: Standards Press of China (in Chinese).

Gilly W F, Beman J M, Litvin S Y, et al. 2013. Oceanographic and biological effects of shoaling of the oxygen minimum zone. Annu Rev Mar Sci, 5: 393-420, doi:10.1146/annurev-marine-120710-100849.

Gopinath A, Sindhu R, Nair S M. 2006. Variability of dissolved reactive phosphate and apparent oxygen utilization along the west coast of India. Chem Ecol, 22(2): 113-123, doi:10.1080/02757540600579334.

Guo J Y, Yang X F, Zhao J, et al. 2023. Distributions of dissolved oxygen and apparent oxygen utilization in the Cosmonaut Sea and Amundsen Sea in austral summer 2021. Adv Polar Sci, 34(4): 272-303, doi:10.12429/j.advps.2023.0007.

Han Z B, Hu C Y, Sun W P, et al. 2019. Characteristics of particle fluxes in the Prydz Bay polynya, Eastern Antarctica. Sci China Earth Sci, 62(4): 657-670, doi:10.1007/s11430-018-9285-6.

Helm K P, Bindoff N L, Church J A. 2011. Observed decreases in oxygen content of the global ocean. Geophys Res Lett, 38(23): L23602, doi:10.1029/2011gl049513.

Hewes C D, Reiss C S, Kahru M, et al. 2008. Control of phytoplankton biomass by dilution and mixed layer depth in the western Weddell-Scotia Confluence. Mar Ecol Prog Ser, 366: 15-29, doi:10.3354/meps07515.

Hu J, Xue S Y, Zhao J, et al. 2023. Dynamics of chromophoric dissolved organic matter in a highly productive Amundsen Sea polynya. Mar Chem, 257: 104329, doi:10.1016/j.marchem.2023.104329.

Iida T, Odate T, Fukuchi M. 2013. Long-term trends of nutrients and apparent oxygen utilization south of the polar front in Southern Ocean intermediate water from 1965 to 2008. PLoS One, 8(8): e71766, doi:10.1371/journal.pone.0071766.

Jacobs S, Jenkins A, Hellmer H, et al. 2012. The Amundsen Sea and the Antarctic ice sheet. Oceanography, 25(3): 154-163, doi:10.5670/oceanog.2012.90.

Keeling R E, Körtzinger A, Gruber N. 2010. Ocean deoxygenation in a warming world. Ann Rev Mar Sci, 2: 199-229, doi:10.1146/annurev.marine.010908.163855.

Kim I, Hahm D, Rhee T S, et al. 2016. The distribution of glacial meltwater in the Amundsen Sea, Antarctica, revealed by dissolved helium and neon. J Geophys Res Oceans, 121(3): 1654-1666, doi:10.1002/2015jc011211.

Kim S J, Lee B Y. 2005. Distribution and vertical structures of water masses around the Antarctic continental margin. Ocean Polar Res, 27(3): 277-288, doi:10.4217/opr.2005.27.3.277.

Kim S U, Kim K Y. 2021. Impact of climate change on the primary production and related biogeochemical cycles in the coastal and sea ice zone of the Southern Ocean. Sci Total Environ, 751: 141678, doi:10.1016/j.scitotenv.2020.141678.

Kitade Y, Shimada K, Tamura T, et al. 2014. Antarctic bottom water production from the Vincennes Bay polynya, East Antarctica. Geophys Res Lett, 41(10): 3528-3534, doi:10.1002/2014gl059971.

Kostyleva A V, Mosharov S A, Podymov O I. 2022. Studies of the seasonal variability of oxygen, apparent oxygen utilization, and chlorophyll-*a* in the northeastern part of the Black Sea in 2012. Oceanology, 62(5): 620-629, doi:10.1134/s0001437022050101.

Lee S H, Kim B K, Yun M S, et al. 2012. Spatial distribution of phytoplankton productivity in the Amundsen Sea, Antarctica. Polar Biol, 35(11): 1721-1733, doi:10.1007/s00300-012-1220-5.

Levin L A. 2018. Manifestation, drivers, and emergence of open ocean deoxygenation. Ann Rev Mar Sci, 10: 229-260, doi:10.1146/annurev-marine-121916-063359.

Li H, Li B R, Guo X J, et al. 2024. An study on the change characteristics of summer hydrographic structure in the Cosmonaut Sea. Mar Sci Bull, 43(1): 21-34, doi:10.11840/j.issn.1001-6392.2024.01.002 (in Chinese with English abstract).

Ludescher J, Yuan N M, Bunde A. 2019. Detecting the statistical significance of the trends in the Antarctic sea ice extent: an indication for a turning point. Clim Dyn, 53(1): 237-244, doi:10.1007/s00382-018-4579-3.

Martinson D G, Iannuzzi R A. 2013. Antarctic ocean-ice interaction: Implications from ocean bulk property distributions in the Weddell Gyre//Jeffries M O (ed.). Antarctic sea ice: physical processes, interactions and variability, 243-271, doi:10.1029/AR074p0243.

Matear R J, Hirst A C, McNeil B I. 2000. Changes in dissolved oxygen in the Southern Ocean with climate change. Geochem Geophys Geosyst, 1(11): 2000GC000086, doi:10.1029/2000gc000086.

McClish S, Bushinsky S M. 2023. Majority of Southern Ocean seasonal sea ice zone bloom net community production precedes total ice retreat. Geophys Res Lett, 50(20): e2023GL103459, doi:10.1029/2023gl103459.

Meijers A J S, Klocker A, Bindoff N L, et al. 2010. The circulation and water masses of the Antarctic shelf and continental slope between 30 and 80°E. Deep Sea Res Part II Top Stud Oceanogr, 57(9/10): 723-737, doi:10.1016/j.dsr2.2009.04.019.

Mendes C R B, de Souza M S, Garcia V M T, et al. 2012. Dynamics of phytoplankton communities during late summer around the tip of the

Antarctic Peninsula. Deep Sea Res Part I Oceanogr Res Pap, 65: 1-14, doi:10.1016/j.dsr.2012.03.002.

Moreau S, Hattermann T, de Steur L, et al. 2023. Wind-driven upwelling of iron sustains dense blooms and food webs in the eastern Weddell Gyre. Nat Commun, 14(1): 1303, doi:10.1038/s41467-023-36992-1.

Mou W X, Yang G, Hao Q, et al. 2021. The zooplankton community in Cosmonaut Sea: community structure and environmental factors. Oceanol Limnol Sin, 52(4): 925-935, doi:10.11693/hyhz20210200043 (in Chinese with English abstract).

Nakayama Y, Menemenlis D, Zhang H, et al. 2018. Origin of Circumpolar Deep Water intruding onto the Amundsen and Bellingshausen Sea continental shelves. Nat Commun, 9: 3403, doi:10.1038/s41467-018-05813-1.

Nielsen J M, Pelland N A, Bell S W, et al. 2023. Seasonal dynamics of primary production in the southeastern Bering Sea assessed using continuous temporal and vertical dissolved oxygen and chlorophyll-*a* measurements. J Geophys Res Oceans, 128(5): e2022JC019076, doi:10.1029/2022jc019076.

Park Y H, Charriaud E, Fieux M. 1998. Thermohaline structure of the Antarctic surface water/winter water in the Indian sector of the Southern Ocean. J Mar Syst, 17(1-4): 5-23, doi:10.1016/S0924-7963(98)00026-8.

Park Y H, Charriaud E, Craneguy P, et al. 2001. Fronts, transport, and Weddell Gyre at 30°E between Africa and Antarctica. J Geophys Res Oceans, 106(C2): 2857-2879, doi:10.1029/2000jc900087.

Pinkerton M H, Décima M, Kitchener J A, et al. 2020. Zooplankton in the Southern Ocean from the continuous plankton recorder: Distributions and long-term change. Deep Sea Res Part I Oceanogr Res Pap, 162: 103303, doi:10.1016/j.dsr.2020.103303.

Purkey S G, Johnson G C. 2013. Antarctic bottom water warming and freshening: contributions to sea level rise, ocean freshwater budgets, and global heat gain. J Clim, 26(16): 6105-6122, doi:10.1175/jcli-d-12-00834.1.

Raiswell R, Hawkings J R, Benning L G, et al. 2016. Potentially bioavailable iron delivery by iceberg-hosted sediments and atmospheric dust to the polar oceans. Biogeosciences, 13(13): 3887-3900, doi:10.5194/bg-13-3887-2016.

Rintoul S R, da Silva C E. 2019. Antarctic circumpolar current//Cochran J K, Bokuniewicz H J, Yager P L. Encyclopedia of ocean sciences (third edition). Cambridge: Academic Press, 248-261, doi:10.1016/978-0-12-409548-9.11298-9.

Schmidtko S, Stramma L, Visbeck M. 2017. Decline in global oceanic oxygen content during the past five decades. Nature, 542(7641): 335-339, doi:10.1038/nature21399.

Solodoch A, Stewart A L, Hogg A M, et al. 2022. How does Antarctic bottom water cross the Southern Ocean? Geophys Res Lett, 49(7): e2021GL097211, doi:10.1029/2021gl097211.

Stammerjohn S E, Martinson D G, Smith R C, et al. 2008. Trends in Antarctic annual sea ice retreat and advance and their relation to El Niño–Southern Oscillation and Southern Annular Mode variability. J Geophys Res, 113(C3): C03S90, doi:10.1029/2007jc004269.

Swadling K M, Kawaguchi S, Hosie G W. 2010. Antarctic mesozooplankton community structure during BROKE-West (30°E–80°E), January–February 2006. Deep Sea Res Part II Top Stud Oceanogr, 57(9/10): 887-904, doi:10.1016/j.dsr2.2008.10.041.

Tagliabue A, Bopp L, Aumont O. 2009. Evaluating the importance of atmospheric and sedimentary iron sources to Southern Ocean biogeochemistry. Geophys Res Lett, 36(13): L13601, doi:10.1029/2009gl038914.

Tamura T, Ohshima K I, Nihashi S. 2008. Mapping of sea ice production for Antarctic coastal polynyas. Geophys Res Lett, 35(7): L07606, doi:10.1029/2007gl032903.

Wang B, Fan L, Zheng M F, et al. 2022. Carbon and iron uptake by phytoplankton in the Amundsen Sea, Antarctica. Biology, 11(12): 1760, doi:10.3390/biology11121760.

Welschmeyer N A. 1994. Fluorometric analysis of chlorophyll *a* in the presence of chlorophyll *b* and pheopigments. Limnol Oceanogr, 39(8): 1985-1992, doi:10.4319/lo.1994.39.8.1985.

Westwood K J, Brian Griffiths F, Meiners K M, et al. 2010. Primary productivity off the Antarctic coast from 30°–80°E; BROKE-West survey, 2006. Deep Sea Res Part II Top Stud Oceanogr, 57(9/10): 794-814, doi:10.1016/j.dsr2.2008.08.020.

Williams G D, Nicol S, Aoki S, et al. 2010. Surface oceanography of BROKE-West, along the Antarctic margin of the south-west Indian Ocean (30–80°E). Deep Sea Res Part II Top Stud Oceanogr, 57(9/10): 738-757, doi:10.1016/j.dsr2.2009.04.020.

Xing S, Hou X L, Shi K L, et al. 2020. Circulation of Circumpolar Deep Water and marine environment traced by $^{127}$I and $^{129}$I speciation in the Amundsen Sea Polynya, Antarctica. J Environ Radioact, 225: 106424, doi:10.1016/j.jenvrad.2020.106424.

Yang G, Li C L, Sun S. 2011. Inter-annual variation in summer zooplankton community structure in Prydz Bay, Antarctica, from 1999 to 2006. Polar Biol, 34(6): 921-932, doi:10.1007/s00300-010-0948-z.

Zhang C, Li S L. 2023. Causes of the record-low Antarctic sea-ice in austral summer 2022. Atmos Ocean Sci Lett, 16(6): 100353, doi:10.1016/j.aosl.2023.100353.

Zhang R, Blain S, Baudet C, et al. 2024. Tagging of water masses with covariance of trace metals and prokaryotic taxa in the Southern Ocean. Limnol Oceanogr Lett, doi:10.1002/lol2.10429.

Zhang W, Hao Q, He J F, et al. 2022. Variability of size-fractionated phytoplankton standing stock in the Amundsen Sea during summer. Adv Polar Sci, 33(1): 1-13, doi:10.13679/j.advps.2021.0035.

# Supplementary Tables and Figures

**Table S1** Measured, average concentration, and standard deviation of DO in the samples from the 66 parallel sample stations

| Station | Depth/m | Measured A/(μmol·L$^{-1}$) | Measured B/(μmol·L$^{-1}$) | Average/(μmol·L$^{-1}$) | Standard deviation/(μmol·L$^{-1}$) |
|---|---|---|---|---|---|
| AM4 | 0 | 717.5 | 720.6 | 719.1 | 2.2 |
| RA1-00 | 150 | 588.8 | 586.3 | 587.5 | 1.8 |
| RA1-01 | 500 | 377.5 | 379.4 | 378.4 | 1.3 |
| RA1-02 | 1000 | 396.3 | 396.3 | 396.3 | <0.1 |
| RA1-03 | 2000 | 423.8 | 424.4 | 424.1 | 0.4 |
| RA1-04 | 3000 | 435.0 | 435.6 | 435.3 | 0.4 |
| RA2-01 | 200 | 618.8 | 618.1 | 618.4 | 0.4 |
| RA2-02 | 200 | 566.9 | 565.0 | 565.9 | 1.3 |
| RA2-03 | 200 | 611.3 | 613.1 | 612.2 | 1.3 |
| RA2-04 | 200 | 442.5 | 440.0 | 441.3 | 1.8 |
| RA3-02 | 500 | 506.3 | 507.5 | 506.9 | 0.9 |
| RA3-03 | 75 | 599.4 | 601.3 | 600.3 | 1.3 |
| RA3-04 | 50 | 609.4 | 609.4 | 609.4 | <0.1 |
| RA4-00 | 200 | 545.6 | 547.5 | 546.6 | 1.3 |
| RA4-01 | 0 | 750.6 | 751.9 | 751.3 | 0.9 |
| RA4-02 | 150 | 485.0 | 482.5 | 483.8 | 1.8 |
| RA4-03 | 25 | 715.6 | 718.1 | 716.9 | 1.8 |
| A1-01 | 200 | 564.4 | 566.3 | 565.3 | 1.3 |
| A1-02 | 200 | 516.9 | 516.3 | 516.6 | 0.4 |
| A1-03 | 200 | 430.0 | 428.8 | 429.4 | 0.9 |
| A2-02 | 200 | 570.0 | 569.4 | 569.7 | 0.4 |
| A2-03 | 200 | 491.9 | 492.5 | 492.2 | 0.4 |
| A2-04 | 200 | 427.5 | 426.9 | 427.2 | 0.4 |
| A9-00 | 200 | 585.6 | 586.9 | 586.3 | 0.9 |
| A9-01 | 200 | 581.9 | 581.9 | 581.9 | <0.1 |
| A9-02 | 200 | 569.4 | 569.4 | 569.4 | <0.1 |
| A9-03 | 200 | 583.8 | 585.0 | 584.4 | 0.9 |
| A11-00 | 200 | 556.9 | 557.5 | 557.2 | 0.4 |
| A11-01 | 200 | 556.9 | 557.5 | 557.2 | 0.4 |
| A11-02 | 200 | 607.5 | 609.4 | 608.4 | 1.3 |
| A11-03 | 200 | 583.8 | 581.9 | 582.8 | 1.3 |
| A11-04 | 200 | 580.6 | 583.1 | 581.9 | 1.8 |
| RAXZ1 | 200 | 718.1 | 721.3 | 719.7 | 2.2 |
| RAXZ2 | 200 | 669.4 | 668.1 | 668.8 | 0.9 |
| C2'-06 | 75 | 602.9 | 598.1 | 600.5 | 3.4 |
| C2'-08 | 40 | 524.4 | 524.2 | 524.3 | 0.2 |
| C2'-11 | 25 | 624.5 | 620.0 | 622.3 | 3.2 |
| C2'-13 | 100 | 628.2 | 625.7 | 626.9 | 1.8 |
| C4-12 | 50 | 600.3 | 594.9 | 597.6 | 3.8 |
| C4-11 | 75 | 599.9 | 596.9 | 598.4 | 2.1 |
| C5'-09 | 100 | 610.7 | 608.3 | 609.5 | 1.7 |
| C5'-07 | 150 | 529.4 | 526.4 | 527.9 | 2.1 |

Continued

| Station | Depth/m | Measured A/(μmol·L$^{-1}$) | Measured B/(μmol·L$^{-1}$) | Average/(μmol·L$^{-1}$) | Standard deviation/(μmol·L$^{-1}$) |
|---|---|---|---|---|---|
| C4-07 | 150 | 377.9 | 373.4 | 375.6 | 3.2 |
| C4-03 | 150 | 363.4 | 364.5 | 363.9 | 0.8 |
| C5'-02 | 75 | 409.2 | 409.6 | 409.4 | 0.3 |
| C5'-00 | 200 | 364.7 | 362.8 | 363.7 | 1.3 |
| C4-00 | 75 | 668.1 | 662.6 | 665.3 | 3.9 |
| C4-01 | 150 | 382.3 | 383.6 | 382.9 | 0.9 |
| C4-02 | 1000 | 404.1 | 408.8 | 406.4 | 3.3 |
| C5-00 | 500 | 352.1 | 355.5 | 353.8 | 2.4 |
| C5-01 | 25 | 709.1 | 709.5 | 709.3 | 0.3 |
| C5-02 | 100 | 617.1 | 617.2 | 617.1 | 0.1 |
| C5-03 | 200 | 492.6 | 491.4 | 492.0 | 0.9 |
| C5-05 | 300 | 461.8 | 460.1 | 460.9 | 1.2 |
| C5-08 | 150 | 627.8 | 624.2 | 626.0 | 2.5 |
| CA1-10 | 25 | 729.5 | 725.3 | 727.4 | 3.0 |
| CA2-07 | 1000 | 439.6 | 437.1 | 438.4 | 1.8 |
| CA1-07 | 200 | 624.2 | 625.3 | 624.7 | 0.8 |
| CA2-06 | 50 | 681.3 | 677.0 | 679.1 | 3.1 |
| CA2-05 | 50 | 677.3 | 675.1 | 676.2 | 1.6 |
| C6'-05 | 100 | 582.3 | 578.9 | 580.6 | 2.4 |
| CA3-07 | 809 | 457.7 | 454.6 | 456.1 | 2.2 |
| CA3-08 | 200 | 564.4 | 559.5 | 562.0 | 3.5 |
| CA3-05 | 150 | 438.5 | 436.8 | 437.7 | 1.1 |
| C7'-05 | 50 | 543.1 | 544.2 | 543.6 | 0.7 |
| C7-03 | 1000 | 400.6 | 398.7 | 399.7 | 1.4 |

**Table S2** The concentrations of dissolved oxygen (DO) and apparent oxygen utilization (AOU) in the Cosmonaut Sea of the whole water depth

| Station | Longitude | Latitude | Bottom depth/m | Sample depth/m | DO/(μmol·L$^{-1}$) | AOU/(μmol·L$^{-1}$) |
|---|---|---|---|---|---|---|
| C2'-06 | 34.17°E | 65.19°S | 1503 | 5 | 712.8 | −0.3 |
| | | | | 25 | 719.3 | 7.2 |
| | | | | 50 | 662.1 | 41.9 |
| | | | | 75 | 600.5 | 77.5 |
| | | | | 100 | 587.6 | 83.0 |
| | | | | 150 | 544.9 | 98.2 |
| | | | | 200 | 483.6 | 120.0 |
| | | | | 300 | 414.0 | 146.5 |
| | | | | 500 | 406.0 | 149.2 |
| | | | | 1000 | 406.4 | 152.1 |
| | | | | 1492 | 415.9 | 150.1 |
| C2'-08 | 34.01°E | 65.55°S | 3215 | 5 | 723.5 | −5.3 |
| | | | | 25 | 714.0 | 9.6 |
| | | | | 40 | 696.7 | 20.8 |
| | | | | 50 | 658.1 | 45.1 |
| | | | | 75 | 614.7 | 70.4 |
| | | | | 100 | 602.0 | 75.7 |

Continued

| Station | Longitude | Latitude | Bottom depth/m | Sample depth/m | DO/(μmol·L$^{-1}$) | AOU/(μmol·L$^{-1}$) |
|---|---|---|---|---|---|---|
| | | | | 150 | 524.3 | 103.3 |
| | | | | 200 | 472.4 | 121.9 |
| | | | | 300 | 404.8 | 149.0 |
| | | | | 500 | 413.1 | 146.1 |
| | | | | 1000 | 416.1 | 146.6 |
| | | | | 2000 | 447.8 | 135.6 |
| | | | | 3000 | 468.4 | 127.6 |
| | | | | 3215 | 472.5 | 125.9 |
| C2'-09 | 33.57°E | 66.01°S | 1125 | 5 | 731.7 | −6.1 |
| | | | | 25 | 731.6 | 2.1 |
| | | | | 36 | 683.5 | 31.7 |
| | | | | 50 | 617.8 | 69.8 |
| | | | | 75 | 601.3 | 78.0 |
| | | | | 100 | 601.1 | 77.9 |
| | | | | 150 | 590.6 | 82.5 |
| | | | | 200 | 558.8 | 93.2 |
| | | | | 300 | 448.3 | 134.9 |
| | | | | 500 | 402.7 | 152.3 |
| | | | | 1000 | 411.5 | 152.1 |
| | | | | 1118 | 408.1 | 154.3 |
| C2'-11 | 33.50°E | 66.65°S | 1168 | 5 | 720.0 | 4.5 |
| | | | | 25 | 676.4 | 37.5 |
| | | | | 50 | 626.0 | 65.7 |
| | | | | 75 | 622.3 | 67.7 |
| | | | | 100 | 613.5 | 72.0 |
| | | | | 150 | 602.4 | 77.1 |
| | | | | 200 | 593.3 | 81.1 |
| | | | | 300 | 523.5 | 106.7 |
| | | | | 500 | 408.5 | 149.4 |
| | | | | 1000 | 412.1 | 151.5 |
| | | | | 1158 | 417.9 | 149.5 |
| C2'-13 | 33.30°E | 67.25°S | 1103 | 5 | 790.8 | −31.5 |
| | | | | 25 | 690.6 | 22.8 |
| | | | | 50 | 638.8 | 59.4 |
| | | | | 75 | 630.4 | 63.5 |
| | | | | 100 | 626.9 | 65.1 |
| | | | | 150 | 615.0 | 70.8 |
| | | | | 200 | 610.9 | 72.2 |
| | | | | 300 | 558.8 | 91.2 |
| | | | | 500 | 430.6 | 139.1 |
| | | | | 1000 | 443.0 | 137.3 |
| | | | | 1096 | 429.7 | 143.9 |
| C4-00 | 44.94°E | 62.01°S | 4915 | 5 | 714.1 | −1.4 |
| | | | | 25 | 708.4 | 1.4 |
| | | | | 50 | 693.2 | 10.2 |

Continued

| Station | Longitude | Latitude | Bottom depth/m | Sample depth/m | DO/(μmol·L$^{-1}$) | AOU/(μmol·L$^{-1}$) |
|---|---|---|---|---|---|---|
| | | | | 75 | 665.3 | 44.6 |
| | | | | 100 | 575.2 | 80.2 |
| | | | | 150 | 405.2 | 145.3 |
| | | | | 200 | 367.6 | 160.2 |
| | | | | 300 | 373.1 | 157.6 |
| | | | | 500 | 427.8 | 131.2 |
| | | | | 1000 | 439.1 | 129.7 |
| | | | | 2000 | 433.6 | 138.9 |
| | | | | 3000 | 448.4 | 134.8 |
| | | | | 4000 | 476.4 | 123.0 |
| | | | | 4990 | 489.0 | 117.5 |
| C4-01 | 45.00°E | 62.66°S | 4631 | 5 | 712.4 | −1.1 |
| | | | | 25 | 709.3 | 1.8 |
| | | | | 50 | 694.6 | 27.7 |
| | | | | 75 | 657.3 | 48.1 |
| | | | | 100 | 505.8 | 105.3 |
| | | | | 150 | 382.9 | 154.4 |
| | | | | 200 | 372.2 | 158.8 |
| | | | | 300 | 376.6 | 156.7 |
| | | | | 500 | 389.7 | 151.5 |
| | | | | 1000 | 395.1 | 153.0 |
| | | | | 2000 | 444.2 | 134.1 |
| | | | | 3000 | 466.2 | 126.2 |
| | | | | 4000 | 487.8 | 117.5 |
| | | | | 4748 | 497.3 | 113.7 |
| C4-02 | 44.99°E | 63.33°S | 4528 | 5 | 698.4 | 5.9 |
| | | | | 25 | 697.4 | 7.8 |
| | | | | 50 | 670.7 | 39.6 |
| | | | | 75 | 544.6 | 104.5 |
| | | | | 100 | 398.6 | 158.8 |
| | | | | 150 | 375.8 | 158.0 |
| | | | | 200 | 370.3 | 159.7 |
| | | | | 300 | 368.8 | 160.6 |
| | | | | 500 | 386.0 | 153.3 |
| | | | | 1000 | 406.4 | 147.4 |
| | | | | 2000 | 426.9 | 142.7 |
| | | | | 3000 | 463.0 | 127.8 |
| | | | | 4000 | 489.2 | 116.8 |
| | | | | 4573 | 489.8 | 117.4 |
| C4-03 | 45.00°E | 64.01°S | 4302 | 5 | 684.0 | 10.3 |
| | | | | 25 | 678.1 | 12.0 |
| | | | | 37 | 674.4 | 14.3 |
| | | | | 50 | 604.4 | 53.3 |
| | | | | 75 | 409.6 | 144.8 |
| | | | | 100 | 369.1 | 162.1 |

Continued

| Station | Longitude | Latitude | Bottom depth/m | Sample depth/m | DO/(μmol·L$^{-1}$) | AOU/(μmol·L$^{-1}$) |
|---|---|---|---|---|---|---|
| | | | | 150 | 363.9 | 163.3 |
| | | | | 200 | 365.8 | 162.1 |
| | | | | 300 | 371.5 | 159.6 |
| | | | | 500 | 386.1 | 154.1 |
| | | | | 1000 | 405.1 | 148.9 |
| C4-05 | 45.00°E | 64.66°S | 3885 | 5 | 688.7 | 10.4 |
| | | | | 25 | 674.5 | 15.7 |
| | | | | 50 | 592.2 | 79.9 |
| | | | | 75 | 525.4 | 105.3 |
| | | | | 100 | 503.2 | 111.1 |
| | | | | 150 | 402.8 | 148.9 |
| | | | | 200 | 409.6 | 145.6 |
| | | | | 300 | 419.5 | 142.0 |
| | | | | 500 | 409.8 | 145.7 |
| | | | | 1000 | 415.8 | 146.7 |
| C4-07 | 45.01°E | 65.33°S | 3499 | 5 | 674.9 | 20.9 |
| | | | | 25 | 674.2 | 23.3 |
| | | | | 30 | 671.7 | 24.6 |
| | | | | 50 | 578.5 | 83.8 |
| | | | | 75 | 461.8 | 128.4 |
| | | | | 100 | 394.1 | 151.8 |
| | | | | 150 | 375.6 | 157.9 |
| | | | | 200 | 370.0 | 159.9 |
| | | | | 300 | 378.9 | 155.9 |
| | | | | 500 | 393.5 | 150.2 |
| | | | | 1000 | 407.0 | 148.1 |
| | | | | 2000 | 435.3 | 139.8 |
| | | | | 3000 | 463.1 | 129.1 |
| | | | | 3522 | 474.2 | 125.0 |
| C4-09 | 45.00°E | 66.00°S | 3206 | 5 | 738.1 | −21.1 |
| | | | | 25 | 593.3 | 81.8 |
| | | | | 50 | 571.4 | 93.4 |
| | | | | 75 | 564.8 | 96.0 |
| | | | | 100 | 507.8 | 108.7 |
| | | | | 150 | 401.9 | 149.2 |
| | | | | 200 | 393.4 | 152.3 |
| | | | | 300 | 380.6 | 156.7 |
| | | | | 500 | 397.0 | 150.1 |
| | | | | 1000 | 413.8 | 146.0 |
| | | | | 2000 | 439.4 | 138.6 |
| | | | | 3000 | 468.5 | 126.9 |
| | | | | 3224 | 465.3 | 128.3 |
| C4-11 | 45.02°E | 66.67°S | 2115 | 5 | 779.6 | −35.3 |
| | | | | 25 | 608.7 | 73.7 |
| | | | | 50 | 606.2 | 76.0 |

Continued

| Station | Longitude | Latitude | Bottom depth/m | Sample depth/m | DO/(μmol·L$^{-1}$) | AOU/(μmol·L$^{-1}$) |
|---|---|---|---|---|---|---|
| | | | | 75 | 598.4 | 80.1 |
| | | | | 100 | 595.8 | 81.4 |
| | | | | 150 | 569.5 | 94.4 |
| | | | | 200 | 572.6 | 92.5 |
| | | | | 300 | 479.0 | 125.0 |
| | | | | 500 | 386.3 | 160.8 |
| | | | | 1000 | 380.4 | 163.7 |
| | | | | 2000 | 448.4 | 135.6 |
| | | | | 2159 | 418.1 | 151.1 |
| C4-12 | 45.00°E | 67.00°S | 1713 | 5 | 774.4 | −29.0 |
| | | | | 25 | 640.8 | 56.1 |
| | | | | 50 | 597.6 | 79.5 |
| | | | | 75 | 588.5 | 84.2 |
| | | | | 100 | 583.8 | 85.7 |
| | | | | 150 | 520.3 | 104.8 |
| | | | | 200 | 445.2 | 134.5 |
| | | | | 300 | 407.7 | 147.8 |
| | | | | 500 | 411.0 | 146.6 |
| | | | | 1000 | 417.3 | 147.1 |
| | | | | 1679 | 431.5 | 142.5 |
| C5'-00 | 47.49°E | 62.00°S | 4943 | 5 | 702.0 | 5.5 |
| | | | | 25 | 698.3 | 7.7 |
| | | | | 50 | 693.5 | 11.0 |
| | | | | 75 | 682.3 | 30.8 |
| | | | | 100 | 604.8 | 67.0 |
| | | | | 150 | 389.3 | 151.9 |
| | | | | 200 | 363.7 | 162.9 |
| | | | | 300 | 350.9 | 167.6 |
| | | | | 500 | 366.4 | 160.8 |
| | | | | 1000 | 393.4 | 151.3 |
| C5-00 | 50.00°E | 62.00°S | 5106 | 5 | 720.2 | −6.3 |
| | | | | 25 | 713.5 | −2.6 |
| | | | | 50 | 709.1 | 1.1 |
| | | | | 75 | 694.3 | 27.2 |
| | | | | 100 | 642.8 | 51.6 |
| | | | | 150 | 411.0 | 143.3 |
| | | | | 200 | 356.1 | 165.1 |
| | | | | 300 | 347.1 | 168.7 |
| | | | | 500 | 353.8 | 165.5 |
| | | | | 1000 | 392.3 | 149.9 |
| C5'-01 | 47.50°E | 62.66°S | 4562 | 5 | 687.3 | 10.3 |
| | | | | 25 | 681.2 | 13.6 |
| | | | | 50 | 664.4 | 23.6 |
| | | | | 75 | 556.3 | 91.8 |
| | | | | 100 | 393.0 | 153.0 |

Continued

| Station | Longitude | Latitude | Bottom depth/m | Sample depth/m | DO/(μmol·L$^{-1}$) | AOU/(μmol·L$^{-1}$) |
|---|---|---|---|---|---|---|
| | | | | 150 | 363.4 | 164.2 |
| | | | | 200 | 356.7 | 166.4 |
| | | | | 300 | 365.0 | 162.2 |
| | | | | 500 | 381.3 | 155.2 |
| | | | | 1000 | 401.2 | 149.9 |
| C5-01 | 49.99°E | 62.66°S | 4982 | 5 | 716.1 | −6.6 |
| | | | | 25 | 709.3 | −3.1 |
| | | | | 50 | 697.7 | 2.0 |
| | | | | 75 | 692.2 | 7.1 |
| | | | | 100 | 682.0 | 28.3 |
| | | | | 150 | 552.0 | 84.8 |
| | | | | 200 | 396.2 | 149.2 |
| | | | | 300 | 381.3 | 151.8 |
| | | | | 500 | 373.7 | 156.5 |
| C5'-02 | 47.50°E | 63.33°S | 4624 | 5 | 688.7 | 9.6 |
| | | | | 25 | 681.0 | 13.6 |
| | | | | 50 | 662.3 | 23.2 |
| | | | | 75 | 409.4 | 150.8 |
| | | | | 100 | 367.2 | 162.4 |
| | | | | 150 | 354.4 | 167.4 |
| | | | | 200 | 354.8 | 166.9 |
| | | | | 300 | 362.4 | 163.9 |
| | | | | 500 | 371.5 | 160.7 |
| | | | | 1000 | 391.6 | 155.7 |
| C5-02 | 50.00°E | 63.25°S | 4879 | 5 | 717.3 | −5.7 |
| | | | | 25 | 712.7 | −3.3 |
| | | | | 50 | 708.1 | −0.6 |
| | | | | 75 | 664.4 | 45.2 |
| | | | | 100 | 617.1 | 64.0 |
| | | | | 150 | 376.8 | 156.6 |
| | | | | 200 | 371.1 | 158.9 |
| | | | | 300 | 373.2 | 157.5 |
| | | | | 500 | 399.5 | 145.7 |
| | | | | 1000 | 390.9 | 155.2 |
| C5'-03 | 47.48°E | 64.00°S | 4347 | 5 | 691.3 | 9.7 |
| | | | | 25 | 677.1 | 16.7 |
| | | | | 50 | 653.3 | 30.6 |
| | | | | 75 | 509.4 | 113.0 |
| | | | | 100 | 541.2 | 98.4 |
| | | | | 150 | 373.2 | 162.7 |
| | | | | 200 | 367.4 | 164.6 |
| | | | | 300 | 352.7 | 168.9 |
| | | | | 500 | 363.7 | 164.8 |
| | | | | 1000 | 387.8 | 158.1 |
| C5-03 | 49.99°E | 63.99°S | 4411 | 5 | 711.0 | 2.6 |

Continued

| Station | Longitude | Latitude | Bottom depth/m | Sample depth/m | DO/(μmol·L$^{-1}$) | AOU/(μmol·L$^{-1}$) |
|---|---|---|---|---|---|---|
| | | | | 25 | 702.1 | 7.4 |
| | | | | 50 | 686.7 | 17.6 |
| | | | | 75 | 607.3 | 72.9 |
| | | | | 100 | 613.0 | 69.7 |
| | | | | 150 | 535.7 | 96.6 |
| | | | | 200 | 492.0 | 114.1 |
| | | | | 300 | 397.1 | 157.1 |
| | | | | 500 | 402.9 | 147.7 |
| | | | | 1000 | 436.8 | 136.2 |
| C5'-05 | 47.49°E | 64.66°S | 3068 | 5 | 686.7 | 17.3 |
| | | | | 25 | 682.7 | 19.4 |
| | | | | 50 | 666.3 | 28.6 |
| | | | | 75 | 623.3 | 66.8 |
| | | | | 100 | 623.5 | 66.9 |
| | | | | 150 | 601.6 | 74.4 |
| | | | | 200 | 542.7 | 96.4 |
| | | | | 300 | 429.0 | 139.2 |
| | | | | 500 | 416.4 | 144.3 |
| | | | | 1000 | 401.9 | 154.8 |
| C5-05 | 50.00°E | 64.66°S | 3627 | 5 | 715.0 | 3.0 |
| | | | | 25 | 708.2 | 7.9 |
| | | | | 50 | 693.5 | 16.6 |
| | | | | 75 | 617.1 | 67.8 |
| | | | | 100 | 605.0 | 67.5 |
| | | | | 150 | 494.5 | 112.2 |
| | | | | 200 | 443.6 | 132.1 |
| | | | | 300 | 460.9 | 124.9 |
| | | | | 500 | 424.4 | 139.2 |
| | | | | 1000 | 418.7 | 145.8 |
| C5'-07 | 47.48°E | 65.33°S | 2656 | 5 | 697.9 | 9.7 |
| | | | | 25 | 667.6 | 30.1 |
| | | | | 50 | 626.2 | 56.3 |
| | | | | 75 | 605.2 | 75.1 |
| | | | | 100 | 592.6 | 78.3 |
| | | | | 150 | 527.9 | 101.9 |
| | | | | 200 | 418.4 | 141.9 |
| | | | | 300 | 382.4 | 156.0 |
| | | | | 500 | 388.7 | 154.6 |
| | | | | 1000 | 404.6 | 151.6 |
| C5-07 | 50.00°E | 65.33°S | 2116 | 5 | 720.5 | 7.4 |
| | | | | 25 | 714.3 | 10.5 |
| | | | | 50 | 709.1 | 13.2 |
| | | | | 75 | 703.8 | 16.4 |
| | | | | 100 | 626.4 | 64.7 |
| | | | | 150 | 629.2 | 63.2 |

Continued

| Station | Longitude | Latitude | Bottom depth/m | Sample depth/m | DO/(μmol·L$^{-1}$) | AOU/(μmol·L$^{-1}$) |
|---|---|---|---|---|---|---|
| | | | | 200 | 612.5 | 69.0 |
| | | | | 300 | 539.4 | 96.6 |
| | | | | 500 | 467.3 | 124.0 |
| | | | | 1000 | 436.3 | 139.6 |
| | | | | 2096 | 469.0 | 126.9 |
| C5-08 | 50.00°E | 65.67°S | 1862 | 5 | 735.4 | 1.4 |
| | | | | 25 | 725.8 | 6.5 |
| | | | | 50 | 718.9 | 9.9 |
| | | | | 75 | 701.4 | 19.0 |
| | | | | 100 | 657.2 | 47.0 |
| | | | | 150 | 626.0 | 64.8 |
| | | | | 200 | 653.1 | 50.4 |
| | | | | 300 | 585.0 | 76.4 |
| | | | | 500 | 447.4 | 130.2 |
| | | | | 1000 | 457.6 | 129.2 |
| C5'-09 | 47.50°E | 65.99°S | 2634 | 5 | 711.5 | 2.7 |
| | | | | 25 | 693.4 | 15.8 |
| | | | | 50 | 696.2 | 14.9 |
| | | | | 75 | 648.7 | 49.6 |
| | | | | 100 | 609.5 | 73.6 |
| | | | | 150 | 594.1 | 79.1 |
| | | | | 200 | 579.0 | 82.3 |
| | | | | 300 | 378.3 | 158.2 |
| | | | | 500 | 396.1 | 150.1 |
| | | | | 1000 | 410.2 | 147.0 |
| C5-09 | 49.70°E | 66.00°S | 1453 | 5 | 734.7 | 4.8 |
| | | | | 25 | 727.6 | 8.2 |
| | | | | 50 | 709.1 | 17.9 |
| | | | | 75 | 709.6 | 15.7 |
| | | | | 100 | 711.4 | 14.8 |
| | | | | 150 | 639.0 | 58.1 |
| | | | | 200 | 626.5 | 63.8 |
| | | | | 300 | 561.1 | 89.1 |
| | | | | 500 | 486.2 | 116.9 |
| | | | | 1000 | 446.3 | 134.2 |
| C5'-11 | 47.53°E | 66.64°S | 523.7 | 5 | 741.4 | −6.0 |
| | | | | 25 | 746.1 | −7.9 |
| | | | | 50 | 665.0 | 40.3 |
| | | | | 75 | 619.9 | 68.2 |
| | | | | 100 | 607.4 | 74.3 |
| | | | | 150 | 589.6 | 82.6 |
| | | | | 200 | 563.7 | 94.2 |
| | | | | 300 | 526.1 | 110.1 |
| | | | | 500 | 514.0 | 111.0 |
| | | | | 518 | 528.7 | 103.3 |

Continued

| Station | Longitude | Latitude | Bottom depth/m | Sample depth/m | DO/(μmol·L$^{-1}$) | AOU/(μmol·L$^{-1}$) |
|---|---|---|---|---|---|---|
| C6'-05 | 52.5°E | 64.66°S | 2977 | 5 | 674.3 | 22.7 |
| | | | | 25 | 668.9 | 25.6 |
| | | | | 50 | 663.0 | 29.7 |
| | | | | 75 | 596.6 | 78.6 |
| | | | | 100 | 580.6 | 85.4 |
| | | | | 150 | 460.3 | 125.1 |
| | | | | 200 | 429.8 | 141.7 |
| | | | | 300 | 389.4 | 155.8 |
| | | | | 500 | 404.0 | 151.5 |
| | | | | 1000 | 390.3 | 158.8 |
| C6-05 | 55.00°E | 64.67°S | 4096 | 5 | 670.5 | 26.4 |
| | | | | 25 | 661.8 | 30.8 |
| | | | | 50 | 640.5 | 41.9 |
| | | | | 75 | 421.7 | 142.4 |
| | | | | 100 | 387.4 | 159.3 |
| | | | | 150 | 356.2 | 169.6 |
| | | | | 200 | 357.5 | 167.2 |
| | | | | 300 | 350.1 | 170.0 |
| | | | | 500 | 384.7 | 153.9 |
| | | | | 1000 | 404.0 | 149.5 |
| C6'-07 | 52.50°E | 65.33°S | 2896 | 5 | 694.5 | 20.2 |
| | | | | 25 | 688.9 | 23.0 |
| | | | | 50 | 684.1 | 25.4 |
| | | | | 75 | 672.4 | 31.3 |
| | | | | 100 | 627.6 | 60.0 |
| | | | | 150 | 581.4 | 84.5 |
| | | | | 200 | 549.9 | 93.8 |
| | | | | 300 | 519.8 | 100.9 |
| | | | | 500 | 462.1 | 126.5 |
| | | | | 1000 | 422.5 | 146.6 |
| C6-07 | 54.89°E | 65.23°S | 3482 | 5 | 702.0 | 22.6 |
| | | | | 25 | 693.8 | 26.7 |
| | | | | 50 | 665.6 | 39.5 |
| | | | | 75 | 615.3 | 69.2 |
| | | | | 100 | 599.4 | 77.9 |
| | | | | 150 | 575.1 | 88.6 |
| | | | | 200 | 556.9 | 95.9 |
| | | | | 300 | 537.3 | 104.6 |
| | | | | 500 | 535.6 | 104.4 |
| | | | | 1000 | 426.3 | 144.2 |
| C6'-08 | 52.49°E | 65.65°S | 279 | 5 | 722.3 | 14.1 |
| | | | | 25 | 716.4 | 16.9 |
| | | | | 50 | 712.6 | 18.7 |
| | | | | 75 | 707.8 | 20.2 |
| | | | | 100 | 705.4 | 20.6 |

Continued

| Station | Longitude | Latitude | Bottom depth/m | Sample depth/m | DO/(μmol·L$^{-1}$) | AOU/(μmol·L$^{-1}$) |
|---|---|---|---|---|---|---|
| | | | | 150 | 681.8 | 29.7 |
| | | | | 200 | 648.7 | 47.9 |
| | | | | 270 | 590.3 | 80.0 |
| C6-08 | 55.02°E | 65.51°S | 1020 | 5 | 705.4 | 24.4 |
| | | | | 25 | 690.3 | 30.7 |
| | | | | 50 | 677.5 | 34.0 |
| | | | | 75 | 650.9 | 48.7 |
| | | | | 100 | 615.0 | 69.3 |
| | | | | 150 | 592.6 | 81.3 |
| | | | | 200 | 575.0 | 89.7 |
| | | | | 300 | 558.6 | 95.8 |
| | | | | 500 | 451.3 | 135.5 |
| | | | | 1005 | 424.3 | 146.5 |
| C7-03 | 60.18°E | 64.10°S | 4318 | 5 | 676.1 | 17.8 |
| | | | | 25 | 662.1 | 24.7 |
| | | | | 50 | 659.7 | 28.7 |
| | | | | 75 | 525.6 | 101.2 |
| | | | | 100 | 373.3 | 162.3 |
| | | | | 150 | 314.9 | 186.4 |
| | | | | 200 | 324.3 | 181.0 |
| | | | | 300 | 332.8 | 176.6 |
| | | | | 500 | 357.3 | 165.2 |
| | | | | 1000 | 399.7 | 148.9 |
| C7'-05 | 57.49°E | 64.67°S | 3789 | 5 | 662.1 | 31.2 |
| | | | | 25 | 653.9 | 35.4 |
| | | | | 75 | 481.4 | 119.5 |
| | | | | 100 | 431.3 | 140.3 |
| | | | | 150 | 372.3 | 162.0 |
| | | | | 200 | 362.7 | 165.1 |
| | | | | 300 | 357.0 | 166.4 |
| | | | | 500 | 372.1 | 160.6 |
| | | | | 1000 | 380.6 | 161.1 |
| C7-05 | 60.00°E | 64.67°S | 4143 | 5 | 670.9 | 23.0 |
| | | | | 25 | 653.2 | 31.8 |
| | | | | 50 | 641.5 | 39.0 |
| | | | | 75 | 474.9 | 122.8 |
| | | | | 100 | 368.7 | 164.4 |
| | | | | 150 | 338.9 | 174.9 |
| | | | | 200 | 334.0 | 176.3 |
| | | | | 300 | 342.2 | 172.4 |
| | | | | 500 | 358.4 | 165.6 |
| | | | | 1000 | 366.5 | 165.3 |
| C7'-07 | 57.50°E | 65.43°S | 3174 | 5 | 683.4 | 21.1 |
| | | | | 25 | 674.2 | 25.4 |
| | | | | 50 | 660.5 | 32.6 |

Continued

| Station | Longitude | Latitude | Bottom depth/m | Sample depth/m | DO/(μmol·L$^{-1}$) | AOU/(μmol·L$^{-1}$) |
|---|---|---|---|---|---|---|
| | | | | 75 | 594.3 | 80.1 |
| | | | | 100 | 593.1 | 81.1 |
| | | | | 150 | 584.6 | 84.2 |
| | | | | 200 | 542.2 | 102.1 |
| | | | | 300 | 449.7 | 133.4 |
| | | | | 500 | 421.7 | 142.7 |
| | | | | 1000 | 426.3 | 144.8 |
| C7-07 | 60.00°E | 65.33°S | 3898 | 5 | 686.1 | 18.5 |
| | | | | 25 | 674.8 | 24.3 |
| | | | | 43 | 573.7 | 82.8 |
| | | | | 75 | 385.3 | 157.2 |
| | | | | 100 | 353.5 | 168.3 |
| | | | | 150 | 344.7 | 171.5 |
| | | | | 200 | 352.8 | 166.7 |
| | | | | 300 | 346.9 | 170.0 |
| | | | | 500 | 361.2 | 164.0 |
| | | | | 1000 | 391.1 | 153.4 |
| C7'-09 | 57.51°E | 66.00°S | 1558 | 5 | 698.9 | 23.7 |
| | | | | 25 | 700.3 | 22.2 |
| | | | | 50 | 691.3 | 26.1 |
| | | | | 75 | 664.1 | 36.6 |
| | | | | 100 | 637.3 | 51.9 |
| | | | | 150 | 600.3 | 77.3 |
| | | | | 200 | 596.6 | 79.5 |
| | | | | 300 | 561.7 | 93.2 |
| | | | | 500 | 447.6 | 133.7 |
| | | | | 1000 | 416.5 | 149.2 |
| C7-09 | 60.00°E | 66.00°S | 2674 | 5 | 689.6 | 19.5 |
| | | | | 25 | 678.7 | 24.9 |
| | | | | 50 | 672.5 | 28.0 |
| | | | | 75 | 654.0 | 40.9 |
| | | | | 100 | 592.1 | 80.7 |
| | | | | 150 | 556.7 | 95.8 |
| | | | | 200 | 509.7 | 113.3 |
| | | | | 300 | 470.1 | 127.7 |
| | | | | 500 | 412.3 | 149.5 |
| C7-11 | 60.00°E | 66.66°S | 888 | 5 | 721.1 | 15.1 |
| | | | | 25 | 693.9 | 26.4 |
| | | | | 50 | 669.5 | 34.6 |
| | | | | 75 | 648.3 | 43.6 |
| | | | | 100 | 620.1 | 62.6 |
| | | | | 150 | 577.9 | 88.6 |
| | | | | 200 | 564.8 | 93.0 |
| | | | | 300 | 536.4 | 102.7 |
| | | | | 500 | 480.1 | 123.1 |

Continued

| Station | Longitude | Latitude | Bottom depth/m | Sample depth/m | DO/(μmol·L$^{-1}$) | AOU/(μmol·L$^{-1}$) |
|---|---|---|---|---|---|---|
| | | | | 854 | 421.0 | 147.8 |
| CA1-07 | 48.70°E | 65.35°S | 2305 | 5 | 731.8 | 0.5 |
| | | | | 25 | 721.3 | 6.1 |
| | | | | 50 | 702.9 | 15.5 |
| | | | | 75 | 666.0 | 38.2 |
| | | | | 100 | 629.1 | 63.0 |
| | | | | 150 | 633.5 | 61.9 |
| | | | | 200 | 624.7 | 64.3 |
| | | | | 300 | 556.3 | 91.1 |
| | | | | 500 | 417.6 | 142.3 |
| | | | | 1000 | 411.8 | 149.9 |
| CA1-10 | 48.72°E | 66.31°S | 1010 | 5 | 735.6 | 2.3 |
| | | | | 25 | 727.4 | 6.4 |
| | | | | 50 | 698.7 | 21.4 |
| | | | | 75 | 686.6 | 28.2 |
| | | | | 100 | 669.1 | 37.0 |
| | | | | 150 | 634.3 | 57.4 |
| | | | | 200 | 609.9 | 72.1 |
| | | | | 300 | 590.3 | 81.8 |
| | | | | 500 | 477.6 | 123.5 |
| | | | | 1004 | 403.7 | 155.8 |
| CA2-05 | 51.25°E | 64.66°S | 2823 | 5 | 688.3 | 23.5 |
| | | | | 25 | 684.9 | 24.1 |
| | | | | 50 | 676.2 | 27.5 |
| | | | | 75 | 592.7 | 79.7 |
| | | | | 100 | 573.6 | 89.0 |
| | | | | 150 | 618.2 | 61.3 |
| | | | | 200 | 621.9 | 55.5 |
| | | | | 300 | 589.3 | 63.7 |
| | | | | 500 | 419.4 | 146.8 |
| | | | | 1000 | 378.7 | 167.2 |
| CA2-06 | 51.25°E | 65.00°S | 3046 | 5 | 710.4 | 15.0 |
| | | | | 25 | 697.5 | 21.2 |
| | | | | 50 | 679.1 | 30.0 |
| | | | | 75 | 619.9 | 66.5 |
| | | | | 100 | 624.5 | 66.3 |
| | | | | 150 | 610.8 | 71.0 |
| | | | | 200 | 584.6 | 80.6 |
| | | | | 300 | 480.0 | 119.8 |
| | | | | 500 | 442.6 | 134.4 |
| | | | | 1000 | 424.2 | 144.2 |
| CA2-07 | 51.25°E | 65.33°S | 2230 | 5 | 736.9 | 0.4 |
| | | | | 25 | 728.0 | 4.7 |
| | | | | 50 | 722.8 | 7.4 |
| | | | | 75 | 695.1 | 19.8 |

Continued

| Station | Longitude | Latitude | Bottom depth/m | Sample depth/m | DO/(μmol·L$^{-1}$) | AOU/(μmol·L$^{-1}$) |
|---|---|---|---|---|---|---|
| | | | | 100 | 672.1 | 33.3 |
| | | | | 150 | 619.4 | 67.6 |
| | | | | 200 | 575.3 | 84.5 |
| | | | | 300 | 498.8 | 113.3 |
| | | | | 500 | 466.5 | 125.2 |
| | | | | 1000 | 438.4 | 139.0 |
| CA2-09 | 51.22°E | 65.98°S | 248 | 5 | 741.1 | 3.8 |
| | | | | 25 | 731.4 | 8.7 |
| | | | | 50 | 716.9 | 15.6 |
| | | | | 75 | 711.2 | 18.0 |
| | | | | 100 | 700.3 | 22.7 |
| | | | | 150 | 686.3 | 28.6 |
| | | | | 200 | 672.5 | 34.9 |
| | | | | 229 | 612.0 | 69.3 |
| CA3-05 | 53.81°E | 64.69°S | 3464 | 5 | 673.9 | 22.8 |
| | | | | 25 | 668.5 | 25.5 |
| | | | | 50 | 661.6 | 29.0 |
| | | | | 75 | 572.9 | 84.5 |
| | | | | 100 | 496.1 | 114.6 |
| | | | | 150 | 437.7 | 137.2 |
| | | | | 200 | 393.5 | 152.1 |
| | | | | 300 | 378.8 | 156.8 |
| | | | | 500 | 398.7 | 149.3 |
| | | | | 1000 | 411.6 | 147.6 |
| CA3-07 | 53.71°E | 65.33°S | 809 | 5 | 690.0 | 21.5 |
| | | | | 25 | 647.1 | 42.7 |
| | | | | 50 | 685.2 | 24.0 |
| | | | | 75 | 684.0 | 24.8 |
| | | | | 100 | 591.0 | 75.1 |
| | | | | 150 | 524.2 | 105.5 |
| | | | | 200 | 430.0 | 140.1 |
| | | | | 300 | 394.7 | 150.8 |
| | | | | 500 | 455.1 | 128.1 |
| | | | | 809 | 456.1 | 130.1 |
| CA3-08 | 53.83°E | 65.55°S | 238 | 5 | 712.8 | 19.2 |
| | | | | 25 | 705.8 | 22.6 |
| | | | | 50 | 693.7 | 26.2 |
| | | | | 75 | 670.6 | 32.5 |
| | | | | 100 | 649.4 | 42.1 |
| | | | | 150 | 576.6 | 88.7 |
| | | | | 200 | 562.0 | 95.8 |
| | | | | 240 | 548.7 | 100.7 |
| MC5-06 | 52.60°E | 65.00°S | 2766 | 5 | 690.0 | 19.5 |
| | | | | 25 | 680.1 | 24.7 |
| | | | | 50 | 678.3 | 25.7 |

Continued

| Station | Longitude | Latitude | Bottom depth/m | Sample depth/m | DO/(μmol·L$^{-1}$) | AOU/(μmol·L$^{-1}$) |
|---|---|---|---|---|---|---|
| | | | | 75 | 668.5 | 31.1 |
| | | | | 100 | 583.6 | 81.6 |
| | | | | 150 | 478.4 | 122.6 |
| | | | | 200 | 458.6 | 129.1 |
| | | | | 300 | 412.7 | 145.4 |
| | | | | 500 | 397.7 | 151.5 |
| | | | | 1000 | 407.0 | 151.5 |
| | | | | 2000 | 438.2 | 141.3 |
| | | | | 2756 | 461.7 | 131.4 |

**Table S3** The concentrations of dissolved oxygen (DO) and apparent oxygen utilization (AOU) in the Amundsen Sea of the whole water depth

| Station | Longitude | Latitude | Bottom depth/m | Sample depth/m | DO/(μmol·L$^{-1}$) | AOU/(μmol·L$^{-1}$) |
|---|---|---|---|---|---|---|
| A1-01 | 129.997°W | 72.99°S | 1533 | 5 | 788.8 | −24.0 |
| | | | | 25 | 777.5 | −14.4 |
| | | | | 50 | 705.0 | 25.6 |
| | | | | 75 | 588.1 | 84.3 |
| | | | | 100 | 582.5 | 87.3 |
| | | | | 150 | 568.1 | 94.1 |
| | | | | 200 | 565.3 | 95.3 |
| | | | | 300 | 541.3 | 105.8 |
| | | | | 500 | 395.6 | 150.4 |
| | | | | 1000 | 425.0 | 139.5 |
| | | | | 1526 | 428.1 | 139.0 |
| A1-02 | 130.062°W | 72.54°S | 2895 | 5 | 775.6 | −14.9 |
| | | | | 25 | 733.8 | 9.6 |
| | | | | 50 | 644.4 | 56.8 |
| | | | | 75 | 625.6 | 66.2 |
| | | | | 100 | 588.8 | 83.8 |
| | | | | 150 | 553.8 | 96.7 |
| | | | | 200 | 516.6 | 108.0 |
| | | | | 300 | 396.3 | 150.3 |
| | | | | 500 | 391.9 | 149.1 |
| | | | | 1000 | 428.8 | 134.7 |
| | | | | 2000 | 453.1 | 126.8 |
| | | | | 2911 | 450.0 | 130.2 |
| A1-03 | 129.846°W | 72.05°S | 3301 | 5 | 779.4 | −13.3 |
| | | | | 25 | 723.8 | 17.1 |
| | | | | 50 | 647.5 | 55.1 |
| | | | | 75 | 608.8 | 72.8 |
| | | | | 100 | 578.1 | 84.7 |
| | | | | 150 | 498.1 | 114.5 |
| | | | | 200 | 429.4 | 138.1 |
| | | | | 300 | 388.8 | 150.6 |
| | | | | 500 | 409.4 | 140.5 |

Continued

| Station | Longitude | Latitude | Bottom depth/m | Sample depth/m | DO/(μmol·L$^{-1}$) | AOU/(μmol·L$^{-1}$) |
|---|---|---|---|---|---|---|
| | | | | 1000 | 430.6 | 133.6 |
| | | | | 2000 | 458.8 | 123.7 |
| | | | | 3000 | 444.4 | 133.0 |
| | | | | 3291 | 453.1 | 129.0 |
| A11-00 | 112.172°W | 73.96°S | 725 | 5 | 791.9 | −27.3 |
| | | | | 25 | 795.0 | −28.6 |
| | | | | 50 | 770.6 | −16.3 |
| | | | | 75 | 606.9 | 70.2 |
| | | | | 100 | 572.5 | 88.9 |
| | | | | 150 | 571.3 | 90.1 |
| | | | | 200 | 557.2 | 96.7 |
| | | | | 300 | 512.5 | 113.9 |
| | | | | 500 | 436.9 | 140.2 |
| | | | | 708 | 415.0 | 147.3 |
| A11-01 | 113.527°W | 73.49°S | 644 | 5 | 797.5 | −33.2 |
| | | | | 25 | 805.6 | −37.2 |
| | | | | 50 | 668.1 | 39.8 |
| | | | | 75 | 630.6 | 61.6 |
| | | | | 100 | 586.3 | 83.3 |
| | | | | 150 | 567.5 | 92.9 |
| | | | | 200 | 574.4 | 88.5 |
| | | | | 300 | 521.9 | 111.8 |
| | | | | 500 | 447.5 | 135.5 |
| | | | | 628 | 410.0 | 149.7 |
| A11-02 | 115.036°W | 72.98°S | 668 | 5 | 797.5 | −32.3 |
| | | | | 25 | 818.1 | −42.6 |
| | | | | 50 | 687.5 | 25.0 |
| | | | | 75 | 640.0 | 55.1 |
| | | | | 100 | 613.1 | 69.9 |
| | | | | 150 | 590.6 | 81.9 |
| | | | | 200 | 608.4 | 73.7 |
| | | | | 300 | 581.9 | 87.9 |
| | | | | 500 | 510.6 | 113.5 |
| | | | | 647 | 437.5 | 136.5 |
| A11-03 | 116.561°W | 72.49°S | 582 | 5 | 837.5 | −46.6 |
| | | | | 10 | 835.0 | −45.4 |
| | | | | 25 | 819.4 | −37.8 |
| | | | | 50 | 684.4 | 27.7 |
| | | | | 75 | 640.6 | 55.9 |
| | | | | 100 | 546.9 | 103.6 |
| | | | | 150 | 589.4 | 83.9 |
| | | | | 200 | 582.8 | 87.4 |
| | | | | 300 | 591.9 | 82.2 |
| | | | | 500 | 445.0 | 135.2 |
| | | | | 568 | 434.4 | 134.6 |

Continued

| Station | Longitude | Latitude | Bottom depth/m | Sample depth/m | DO/(μmol·L$^{-1}$) | AOU/(μmol·L$^{-1}$) |
|---|---|---|---|---|---|---|
| A11-04 | 117.819°W | 72.03°S | 509 | 5 | 805.6 | −28.0 |
| | | | | 25 | 746.3 | 1.8 |
| | | | | 50 | 664.4 | 44.6 |
| | | | | 75 | 590.0 | 83.2 |
| | | | | 100 | 580.0 | 88.5 |
| | | | | 150 | 571.3 | 92.2 |
| | | | | 200 | 581.9 | 87.8 |
| | | | | 300 | 444.4 | 139.7 |
| | | | | 495 | 405.0 | 148.1 |
| A2-02 | 124.388°W | 72.75°S | 456 | 5 | 758.8 | −17.1 |
| | | | | 15 | 774.4 | −20.3 |
| | | | | 25 | 742.5 | −3.8 |
| | | | | 50 | 716.9 | 9.2 |
| | | | | 75 | 673.8 | 35.0 |
| | | | | 100 | 621.9 | 65.3 |
| | | | | 150 | 586.9 | 84.6 |
| | | | | 200 | 569.7 | 94.0 |
| | | | | 300 | 531.9 | 109.4 |
| | | | | 442 | 409.4 | 145.0 |
| A2-03 | 124.940°W | 72.09°S | 2678 | 5 | 782.5 | −18.8 |
| | | | | 25 | 759.4 | −6.2 |
| | | | | 50 | 650.0 | 53.8 |
| | | | | 75 | 615.6 | 70.9 |
| | | | | 100 | 575.0 | 90.3 |
| | | | | 150 | 560.6 | 95.7 |
| | | | | 200 | 492.2 | 121.4 |
| | | | | 300 | 405.6 | 145.5 |
| | | | | 500 | 395.0 | 146.9 |
| | | | | 1000 | 408.8 | 143.9 |
| | | | | 2000 | 453.1 | 126.7 |
| | | | | 2651 | 441.3 | 134.4 |
| A2-04 | 125.803°W | 71.59°S | 3191 | 5 | 759.4 | −2.0 |
| | | | | 25 | 715.6 | 20.4 |
| | | | | 50 | 726.9 | 14.9 |
| | | | | 75 | 615.0 | 69.2 |
| | | | | 100 | 553.8 | 95.4 |
| | | | | 150 | 447.5 | 132.9 |
| | | | | 200 | 427.2 | 136.9 |
| | | | | 300 | 381.3 | 154.0 |
| | | | | 500 | 399.4 | 145.4 |
| | | | | 1000 | 418.8 | 139.4 |
| | | | | 2000 | 445.0 | 130.5 |
| | | | | 3178 | 436.3 | 137.3 |
| A4-03 | 112.735°W | 72.70°S | 431 | 5 | 833.8 | −51.2 |
| | | | | 25 | 732.5 | 0.2 |

Continued

| Station | Longitude | Latitude | Bottom depth/m | Sample depth/m | DO/(μmol·L$^{-1}$) | AOU/(μmol·L$^{-1}$) |
|---|---|---|---|---|---|---|
| | | | | 50 | 603.1 | 74.5 |
| | | | | 75 | 603.1 | 76.0 |
| | | | | 100 | 584.4 | 84.7 |
| | | | | 150 | 567.5 | 91.7 |
| | | | | 200 | 566.3 | 91.2 |
| | | | | 300 | 474.4 | 128.4 |
| | | | | 431 | 424.4 | 144.0 |
| A9-00 | 117.988°W | 73.60°S | 476 | 5 | 813.1 | −45.6 |
| | | | | 25 | 803.1 | −37.2 |
| | | | | 37 | 772.5 | −22.1 |
| | | | | 50 | 786.3 | −26.7 |
| | | | | 75 | 669.4 | 38.5 |
| | | | | 100 | 668.1 | 39.7 |
| | | | | 150 | 600.0 | 78.0 |
| | | | | 200 | 586.3 | 85.5 |
| | | | | 300 | 573.1 | 91.2 |
| | | | | 466 | 466.9 | 130.6 |
| A9-01 | 116.985°W | 73.40°S | 338 | 5 | 823.1 | −52.1 |
| | | | | 25 | 811.9 | −43.0 |
| | | | | 50 | 769.4 | −20.3 |
| | | | | 75 | 771.9 | −17.5 |
| | | | | 100 | 610.0 | 71.8 |
| | | | | 150 | 569.4 | 93.9 |
| | | | | 200 | 581.9 | 87.5 |
| | | | | 300 | 533.1 | 108.4 |
| | | | | 327 | 528.8 | 110.1 |
| A9-02 | 116.013°W | 73.20°S | 678 | 5 | 800.6 | −39.0 |
| | | | | 10 | 793.1 | −35.2 |
| | | | | 25 | 786.3 | −30.7 |
| | | | | 50 | 767.5 | −19.5 |
| | | | | 75 | 661.9 | 39.8 |
| | | | | 100 | 621.9 | 64.2 |
| | | | | 150 | 560.6 | 95.3 |
| | | | | 200 | 569.4 | 91.9 |
| | | | | 300 | 591.3 | 83.3 |
| | | | | 500 | 519.4 | 111.5 |
| | | | | 666 | 453.8 | 130.0 |
| A9-03 | 113.969°W | 72.79°S | 481 | 5 | 850.0 | −56.1 |
| | | | | 25 | 783.8 | −22.5 |
| | | | | 50 | 716.9 | 7.8 |
| | | | | 75 | 608.1 | 72.4 |
| | | | | 100 | 616.3 | 69.1 |
| | | | | 150 | 598.8 | 78.3 |
| | | | | 200 | 584.4 | 83.6 |
| | | | | 300 | 538.1 | 105.0 |

Continued

| Station | Longitude | Latitude | Bottom depth/m | Sample depth/m | DO/(μmol·L$^{-1}$) | AOU/(μmol·L$^{-1}$) |
|---|---|---|---|---|---|---|
| | | | | 451 | 440.0 | 136.0 |
| RA1-00 | 149.888°W | 75.50°S | 3078 | 5 | 761.3 | −6.9 |
| | | | | 25 | 718.1 | 14.3 |
| | | | | 50 | 679.4 | 30.3 |
| | | | | 75 | 573.8 | 91.2 |
| | | | | 100 | 574.4 | 90.8 |
| | | | | 150 | 587.5 | 84.2 |
| | | | | 200 | 581.9 | 86.8 |
| | | | | 300 | 575.6 | 88.2 |
| | | | | 500 | 390.6 | 149.8 |
| | | | | 1000 | 403.1 | 147.8 |
| | | | | 2000 | 440.0 | 133.6 |
| | | | | 3000 | 436.9 | 136.6 |
| | | | | 3083 | 441.3 | 134.4 |
| RA1-01 | 150.100°W | 75.00°S | 3749 | 5 | 726.3 | 2.9 |
| | | | | 25 | 720.6 | 5.0 |
| | | | | 50 | 665.6 | 35.2 |
| | | | | 75 | 558.8 | 99.2 |
| | | | | 100 | 559.4 | 98.7 |
| | | | | 150 | 573.8 | 90.9 |
| | | | | 200 | 579.4 | 87.8 |
| | | | | 300 | 466.3 | 127.2 |
| | | | | 500 | 378.4 | 155.9 |
| | | | | 1000 | 400.6 | 148.6 |
| | | | | 2000 | 421.3 | 142.6 |
| | | | | 3000 | 433.1 | 138.7 |
| | | | | 3726 | 442.5 | 135.3 |
| RA1-02 | 150.024°W | 74.49°S | 3860 | 5 | 740.0 | −1.6 |
| | | | | 25 | 730.6 | 1.9 |
| | | | | 50 | 679.4 | 28.2 |
| | | | | 75 | 566.9 | 94.8 |
| | | | | 100 | 566.9 | 94.7 |
| | | | | 150 | 579.4 | 87.8 |
| | | | | 200 | 591.9 | 81.6 |
| | | | | 300 | 503.8 | 114.0 |
| | | | | 500 | 380.0 | 154.6 |
| | | | | 1000 | 396.3 | 150.6 |
| | | | | 2000 | 425.6 | 140.2 |
| | | | | 3000 | 432.5 | 138.8 |
| | | | | 3850 | 444.4 | 134.5 |
| RA1-03 | 150.035°W | 74.00°S | 4022 | 5 | 721.3 | 4.0 |
| | | | | 25 | 716.9 | 6.2 |
| | | | | 50 | 673.8 | 32.8 |
| | | | | 75 | 563.1 | 95.9 |
| | | | | 100 | 561.3 | 97.6 |

Continued

| Station | Longitude | Latitude | Bottom depth/m | Sample depth/m | DO/(μmol·L$^{-1}$) | AOU/(μmol·L$^{-1}$) |
|---|---|---|---|---|---|---|
| | | | | 150 | 573.8 | 90.2 |
| | | | | 200 | 555.6 | 96.7 |
| | | | | 300 | 409.4 | 145.6 |
| | | | | 500 | 378.1 | 155.6 |
| | | | | 1000 | 391.9 | 152.4 |
| | | | | 2000 | 424.1 | 140.7 |
| | | | | 3000 | 436.3 | 137.2 |
| | | | | 4021 | 446.9 | 133.6 |
| RA1-04 | 149.952°W | 73.01°S | 4129 | 5 | 746.9 | −7.6 |
| | | | | 25 | 728.8 | 1.8 |
| | | | | 50 | 630.0 | 62.6 |
| | | | | 75 | 617.5 | 70.1 |
| | | | | 100 | 595.6 | 78.4 |
| | | | | 150 | 495.6 | 112.7 |
| | | | | 200 | 418.1 | 140.5 |
| | | | | 300 | 381.3 | 153.8 |
| | | | | 500 | 385.0 | 153.0 |
| | | | | 1000 | 396.9 | 150.3 |
| | | | | 2000 | 421.3 | 142.7 |
| | | | | 3000 | 435.3 | 137.9 |
| | | | | 4130 | 451.3 | 131.5 |
| RA2-01 | 144.925°W | 75.01°S | 772 | 5 | 763.1 | −7.3 |
| | | | | 25 | 766.9 | −9.5 |
| | | | | 50 | 715.6 | 16.5 |
| | | | | 75 | 676.3 | 37.5 |
| | | | | 100 | 639.4 | 57.6 |
| | | | | 150 | 618.8 | 69.0 |
| | | | | 200 | 618.4 | 69.1 |
| | | | | 300 | 605.6 | 75.2 |
| | | | | 500 | 509.4 | 108.7 |
| | | | | 763 | 433.1 | 134.0 |
| RA2-02 | 145.040°W | 74.51°S | 3445 | 5 | 740.6 | 0.3 |
| | | | | 25 | 736.3 | 2.5 |
| | | | | 50 | 730.0 | 4.0 |
| | | | | 75 | 588.1 | 84.4 |
| | | | | 100 | 600.6 | 77.9 |
| | | | | 150 | 568.8 | 93.5 |
| | | | | 200 | 565.9 | 92.8 |
| | | | | 300 | 476.3 | 121.5 |
| | | | | 500 | 410.0 | 140.5 |
| | | | | 1000 | 425.0 | 137.1 |
| | | | | 2000 | 440.0 | 133.6 |
| | | | | 3000 | 442.5 | 133.3 |
| | | | | 3425 | 457.5 | 127.3 |
| RA2-03 | 145.172°W | 73.99°S | 3845 | 5 | 723.1 | 8.0 |

Continued

| Station | Longitude | Latitude | Bottom depth/m | Sample depth/m | DO/(μmol·L$^{-1}$) | AOU/(μmol·L$^{-1}$) |
|---|---|---|---|---|---|---|
| | | | | 25 | 722.5 | 8.3 |
| | | | | 50 | 723.8 | 7.9 |
| | | | | 75 | 595.0 | 80.8 |
| | | | | 100 | 591.3 | 81.8 |
| | | | | 150 | 611.3 | 72.8 |
| | | | | 200 | 612.2 | 72.2 |
| | | | | 300 | 458.1 | 128.9 |
| | | | | 500 | 397.5 | 146.2 |
| | | | | 1000 | 422.5 | 137.4 |
| | | | | 2000 | 460.6 | 122.6 |
| | | | | 3000 | 446.3 | 132.1 |
| | | | | 3792 | 451.9 | 130.1 |
| RA2-04 | 145.133°W | 73.00°S | 4024 | 5 | 737.5 | 10.3 |
| | | | | 25 | 743.8 | 7.2 |
| | | | | 35 | 721.9 | 7.2 |
| | | | | 50 | 715.0 | 11.4 |
| | | | | 75 | 595.6 | 79.4 |
| | | | | 100 | 570.0 | 87.0 |
| | | | | 150 | 486.9 | 113.7 |
| | | | | 200 | 441.3 | 127.7 |
| | | | | 300 | 401.9 | 143.0 |
| | | | | 500 | 413.8 | 138.0 |
| | | | | 1000 | 429.4 | 133.7 |
| | | | | 2000 | 437.5 | 134.0 |
| | | | | 3000 | 451.3 | 129.8 |
| | | | | 4012 | 473.1 | 120.2 |
| RA3-02 | 140.036°W | 74.50°S | 558 | 5 | 784.4 | −24.2 |
| | | | | 25 | 772.5 | −19.0 |
| | | | | 50 | 699.4 | 23.6 |
| | | | | 75 | 659.4 | 44.4 |
| | | | | 100 | 636.9 | 56.5 |
| | | | | 150 | 611.9 | 70.4 |
| | | | | 200 | 601.3 | 76.6 |
| | | | | 300 | 576.3 | 88.7 |
| | | | | 500 | 506.9 | 114.0 |
| | | | | 540 | 465.0 | 126.4 |
| RA3-03 | 139.977°W | 73.98°S | 3226 | 5 | 798.8 | −32.1 |
| | | | | 12 | 754.4 | −8.3 |
| | | | | 25 | 721.9 | 14.0 |
| | | | | 50 | 635.6 | 59.2 |
| | | | | 75 | 600.3 | 78.0 |
| | | | | 100 | 582.5 | 86.6 |
| | | | | 150 | 598.1 | 78.6 |
| | | | | 200 | 580.0 | 87.7 |
| | | | | 300 | 502.5 | 115.9 |

Continued

| Station | Longitude | Latitude | Bottom depth/m | Sample depth/m | DO/(μmol·L$^{-1}$) | AOU/(μmol·L$^{-1}$) |
|---|---|---|---|---|---|---|
| | | | | 500 | 383.1 | 153.7 |
| | | | | 1000 | 406.3 | 146.6 |
| | | | | 2000 | 424.4 | 141.6 |
| | | | | 3000 | 438.1 | 136.0 |
| RA3-04 | 140.004°W | 72.99°S | 4015 | 5 | 768.1 | −5.8 |
| | | | | 25 | 733.1 | 11.3 |
| | | | | 50 | 609.4 | 73.9 |
| | | | | 75 | 582.5 | 87.4 |
| | | | | 100 | 551.3 | 100.0 |
| | | | | 150 | 476.9 | 124.1 |
| | | | | 200 | 418.1 | 144.3 |
| | | | | 300 | 375.6 | 156.5 |
| | | | | 500 | 383.8 | 153.0 |
| | | | | 1000 | 396.3 | 150.2 |
| | | | | 2000 | 420.6 | 142.5 |
| | | | | 3000 | 433.1 | 138.9 |
| | | | | 4024 | 441.3 | 135.6 |
| RA4-00 | 135.019°W | 73.49°S | 3146 | 5 | 763.1 | −7.5 |
| | | | | 25 | 738.1 | 5.7 |
| | | | | 50 | 634.4 | 60.3 |
| | | | | 75 | 610.0 | 73.3 |
| | | | | 100 | 578.1 | 88.8 |
| | | | | 150 | 563.8 | 93.8 |
| | | | | 200 | 546.6 | 104.3 |
| | | | | 300 | 417.5 | 144.6 |
| | | | | 500 | 379.4 | 155.2 |
| | | | | 1000 | 440.6 | 128.5 |
| | | | | 2000 | 423.8 | 141.4 |
| | | | | 3000 | 440.0 | 135.5 |
| | | | | 3126 | 453.8 | 129.0 |
| RA4-01 | 135.990°W | 72.97°S | 3632 | 5 | 751.3 | −0.6 |
| | | | | 25 | 730.0 | 13.0 |
| | | | | 50 | 718.8 | 19.1 |
| | | | | 75 | 585.0 | 85.7 |
| | | | | 100 | 562.5 | 94.9 |
| | | | | 150 | 557.5 | 96.0 |
| | | | | 200 | 565.6 | 89.8 |
| | | | | 300 | 410.6 | 146.6 |
| | | | | 500 | 398.8 | 145.6 |
| | | | | 1000 | 413.8 | 141.6 |
| | | | | 2000 | 431.3 | 137.6 |
| | | | | 3000 | 431.9 | 139.3 |
| | | | | 3632 | 440.0 | 136.1 |
| RA4-02 | 134.915°W | 72.53°S | 3856 | 5 | 732.5 | 8.7 |
| | | | | 25 | 736.9 | 8.7 |

Continued

| Station | Longitude | Latitude | Bottom depth/m | Sample depth/m | DO/(μmol·L$^{-1}$) | AOU/(μmol·L$^{-1}$) |
|---|---|---|---|---|---|---|
| | | | | 50 | 646.3 | 55.3 |
| | | | | 75 | 588.1 | 84.3 |
| | | | | 100 | 554.4 | 95.8 |
| | | | | 150 | 483.8 | 119.4 |
| | | | | 200 | 406.9 | 146.7 |
| | | | | 300 | 381.3 | 153.8 |
| | | | | 500 | 391.3 | 149.7 |
| | | | | 1000 | 412.5 | 142.5 |
| | | | | 2000 | 444.4 | 130.7 |
| | | | | 3000 | 436.9 | 137.0 |
| | | | | 3855 | 449.4 | 131.5 |
| RA4-03 | 134.854°W | 72.07°S | 3853 | 5 | 733.8 | 13.4 |
| | | | | 25 | 716.9 | 19.2 |
| | | | | 50 | 618.1 | 69.4 |
| | | | | 75 | 571.3 | 92.0 |
| | | | | 100 | 539.4 | 102.7 |
| | | | | 150 | 480.6 | 120.5 |
| | | | | 200 | 439.4 | 134.6 |
| | | | | 300 | 378.1 | 156.0 |
| | | | | 500 | 378.8 | 155.5 |
| | | | | 1000 | 395.6 | 150.5 |
| | | | | 2000 | 423.1 | 141.2 |
| | | | | 3000 | 435.0 | 137.9 |
| | | | | 3632 | 440.0 | 136.2 |
| RAXZ1 | 138.876°W | 74.94°S | 882 | 5 | 802.5 | −32.8 |
| | | | | 25 | 768.1 | −12.8 |
| | | | | 50 | 733.1 | 5.7 |
| | | | | 75 | 716.3 | 14.4 |
| | | | | 100 | 710.6 | 17.0 |
| | | | | 150 | 718.8 | 12.2 |
| | | | | 200 | 719.7 | 12.0 |
| | | | | 300 | 654.4 | 47.6 |
| | | | | 500 | 521.9 | 108.5 |
| | | | | 855 | 508.1 | 110.7 |
| RAXZ2 | 136.887°W | 74.94°S | 255 | 5 | 804.4 | −39.6 |
| | | | | 15 | 817.5 | −45.5 |
| | | | | 25 | 781.3 | −22.7 |
| | | | | 50 | 726.9 | 8.7 |
| | | | | 75 | 725.0 | 10.7 |
| | | | | 100 | 725.6 | 9.8 |
| | | | | 150 | 726.9 | 9.0 |
| | | | | 200 | 668.8 | 39.2 |
| | | | | 241 | 634.4 | 57.8 |

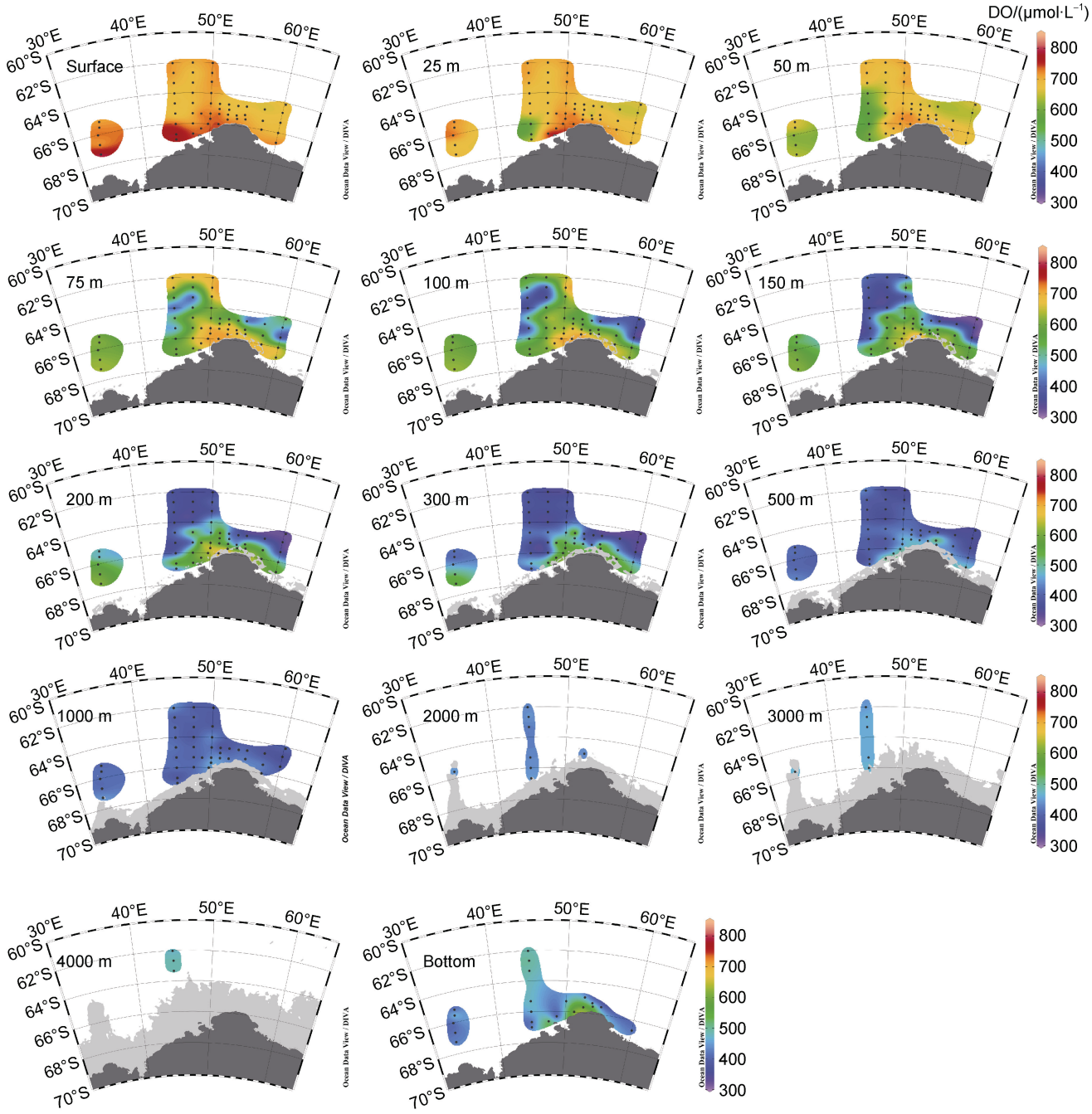


**Figure S1** Horizontal distributions of DO in the Cosmonaut Sea of the whole water depth.

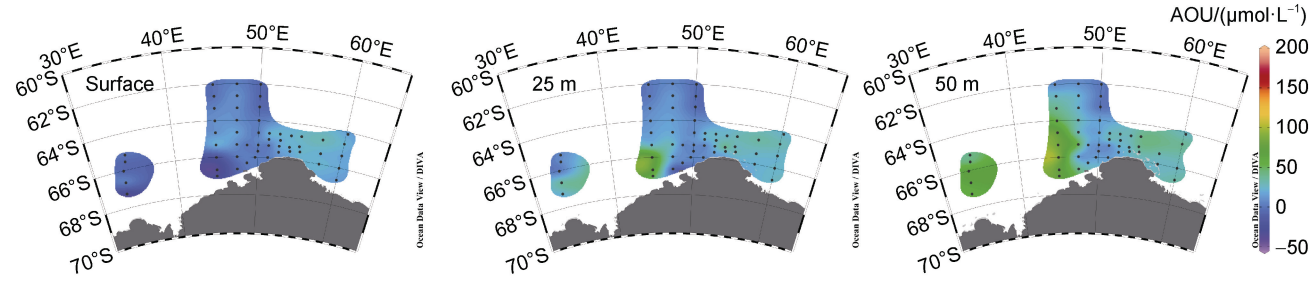

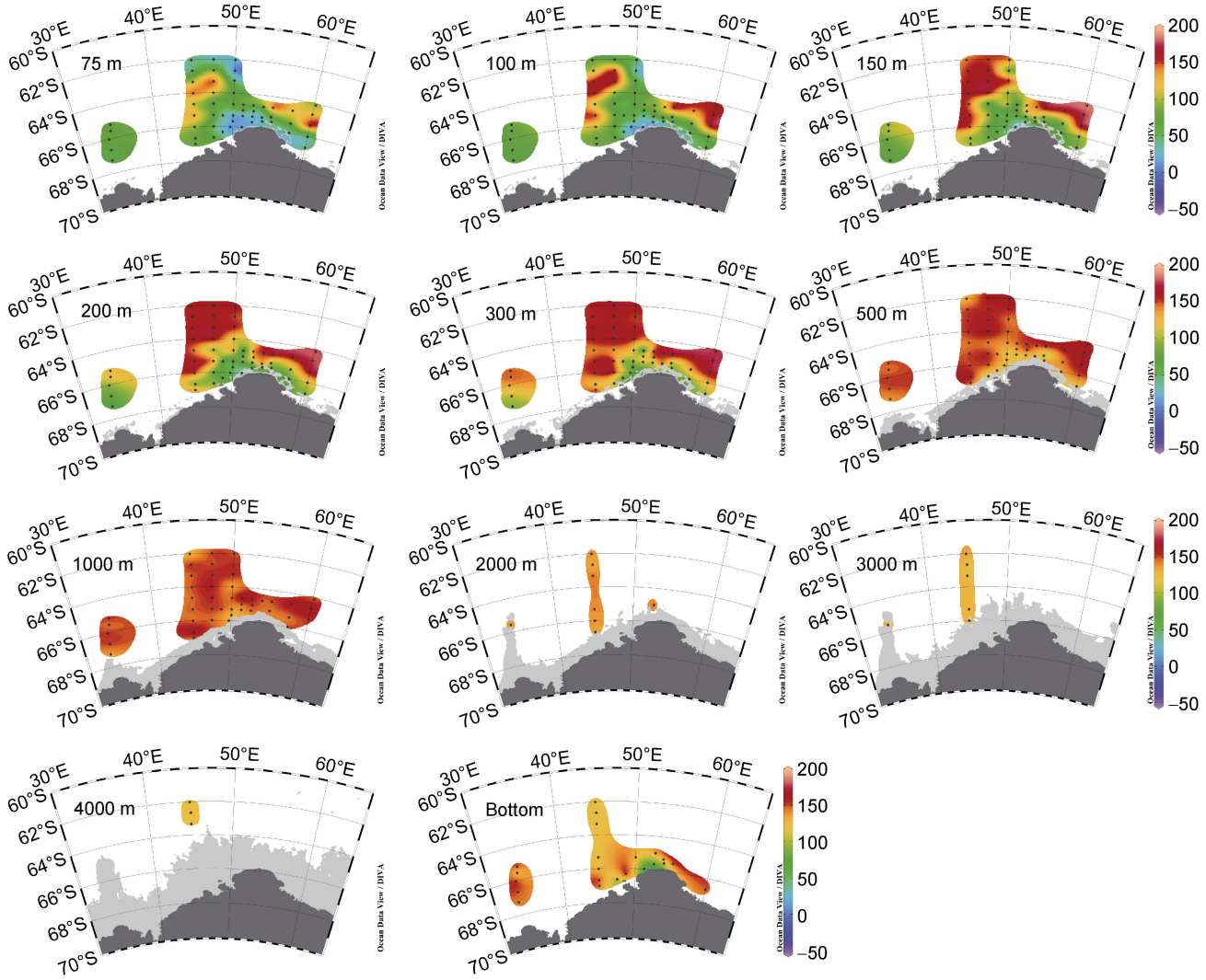


**Figure S2** Horizontal distributions of AOU in the Cosmonaut Sea of the whole water depth.

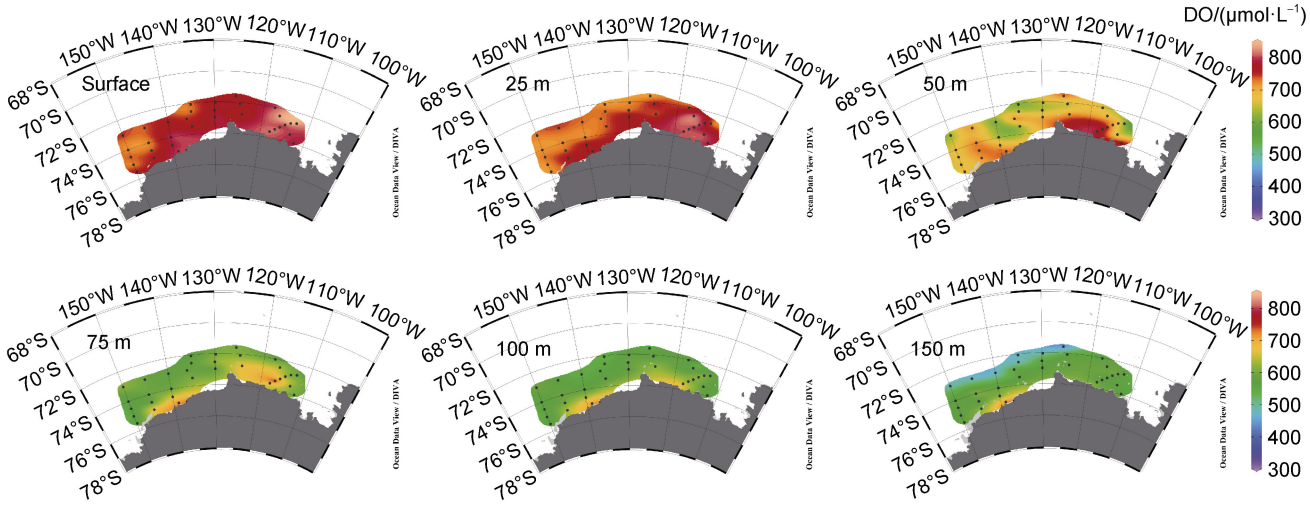

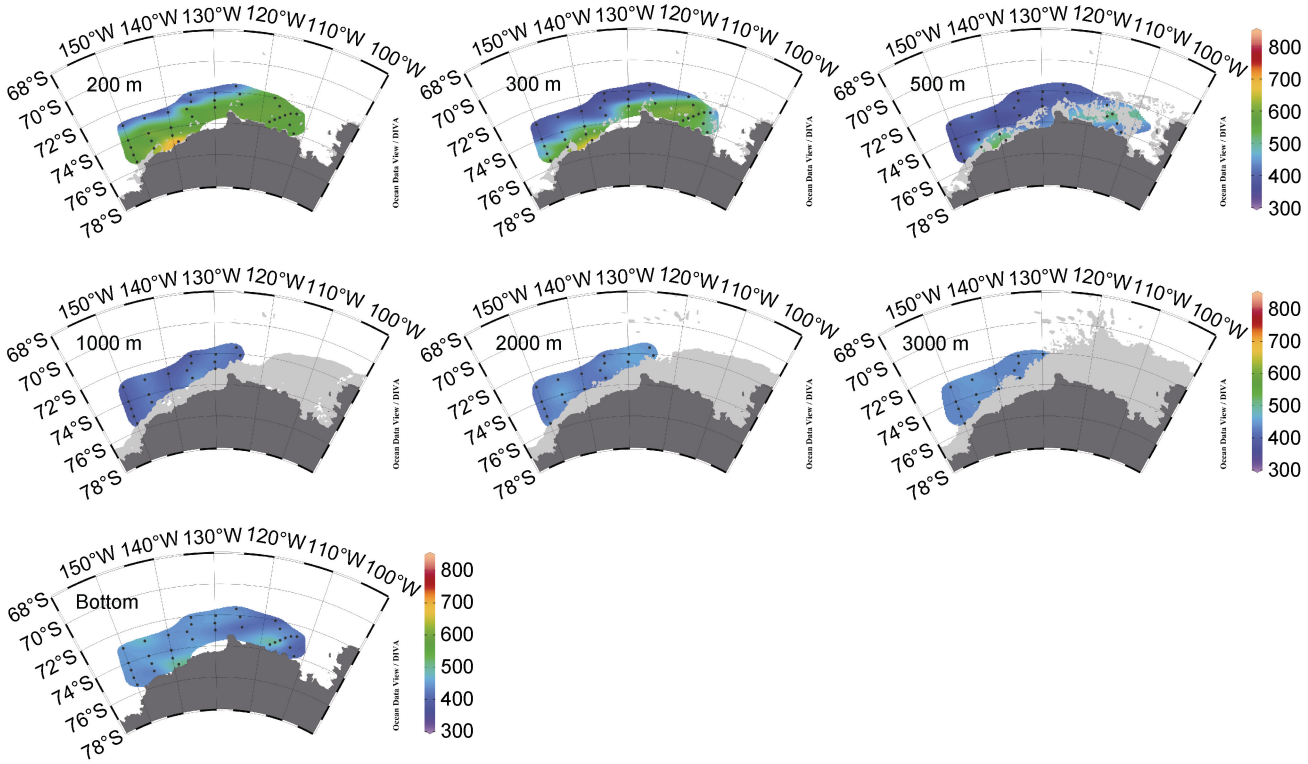


**Figure S3** Horizontal distributions of DO in the Amundsen Sea of the whole water depth.

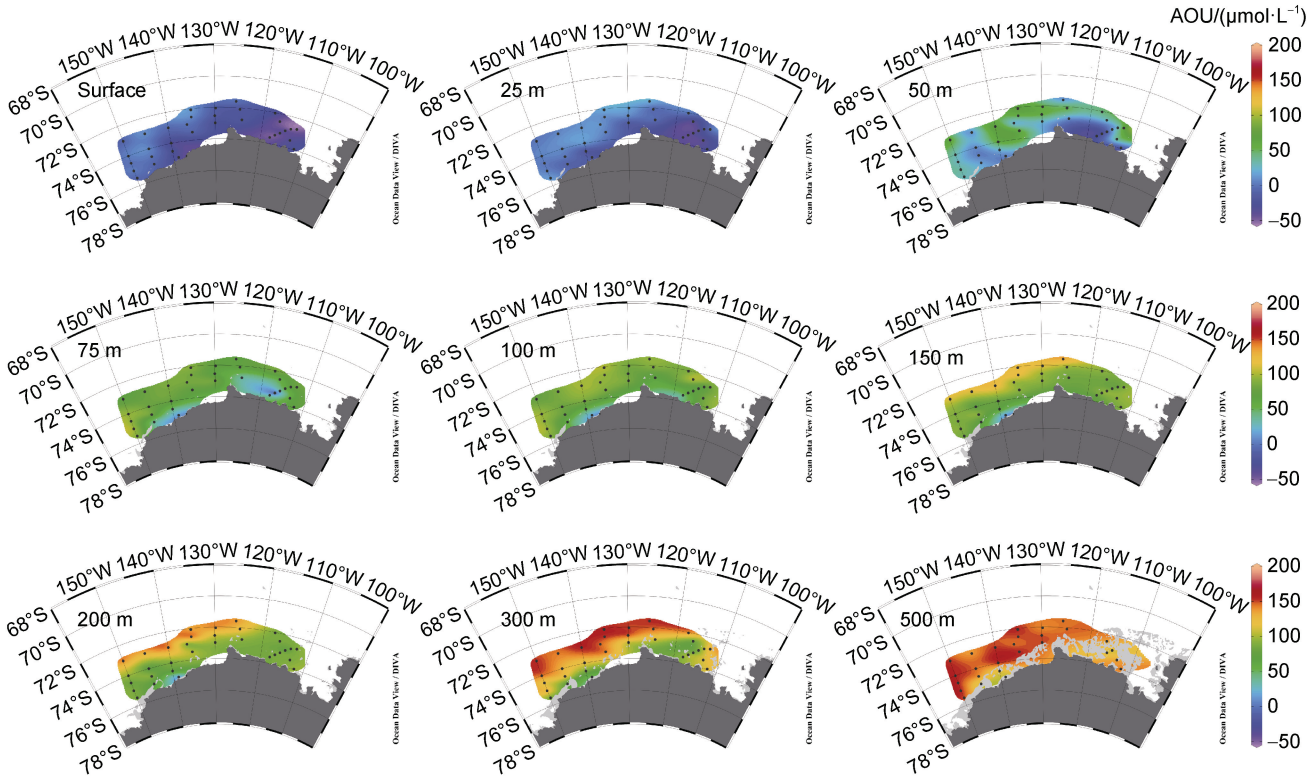

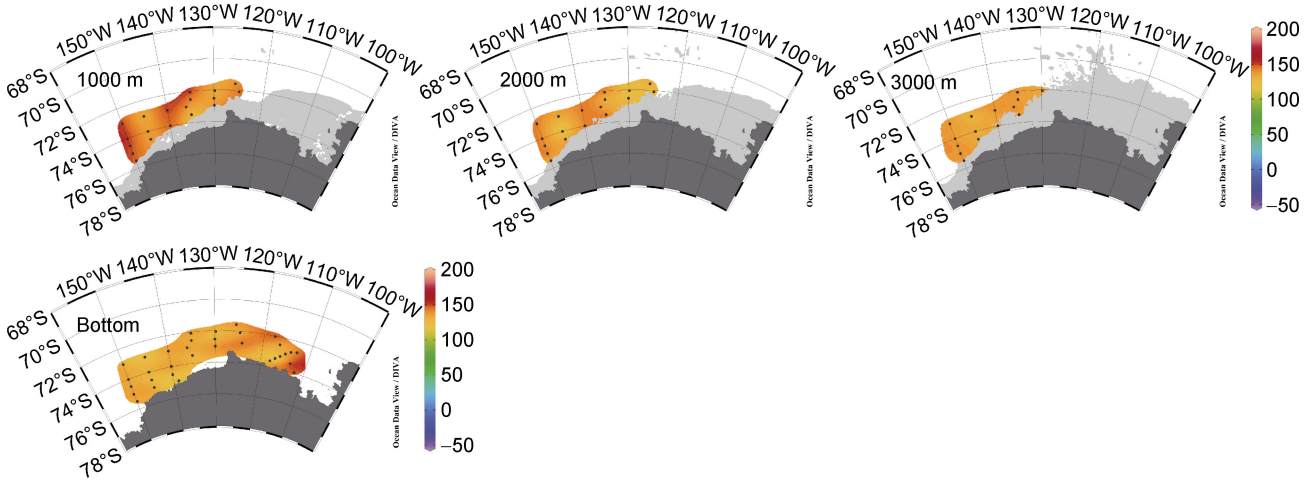


**Figure S4** Horizontal distributions of AOU in the Amundsen Sea of the whole water depth.

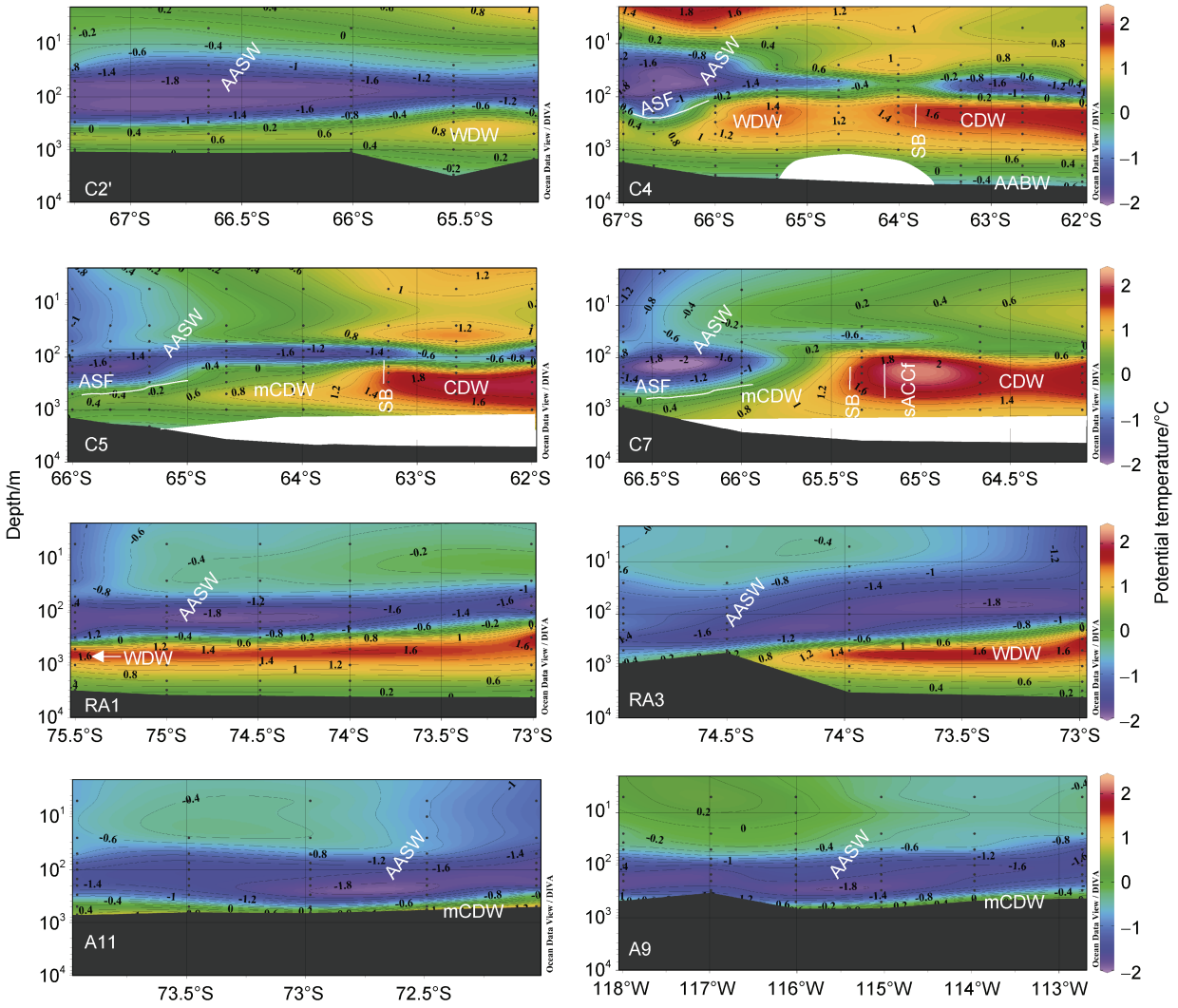


**Figure S5** Vertical distributions of potential temperature (℃) for the whole water depth along transects C2', C4, C5 and C7 in the Cosmonaut Sea and transects RA1, RA3, A11 and A9 in the Amundsen Sea. Major water masses and fronts are labelled as defined in Williams et al. (2020): AASW, Antarctic Surface Water; WDW, Warm Deep Water; CDW, Circumpolar Deep Water; mCDW, modified Circumpolar Deep Water; AABW, Antarctic Bottom Water; SB, Southern Boundary of Antarctic Circumpolar Current. Note: depth was displayed in logarithmic form.

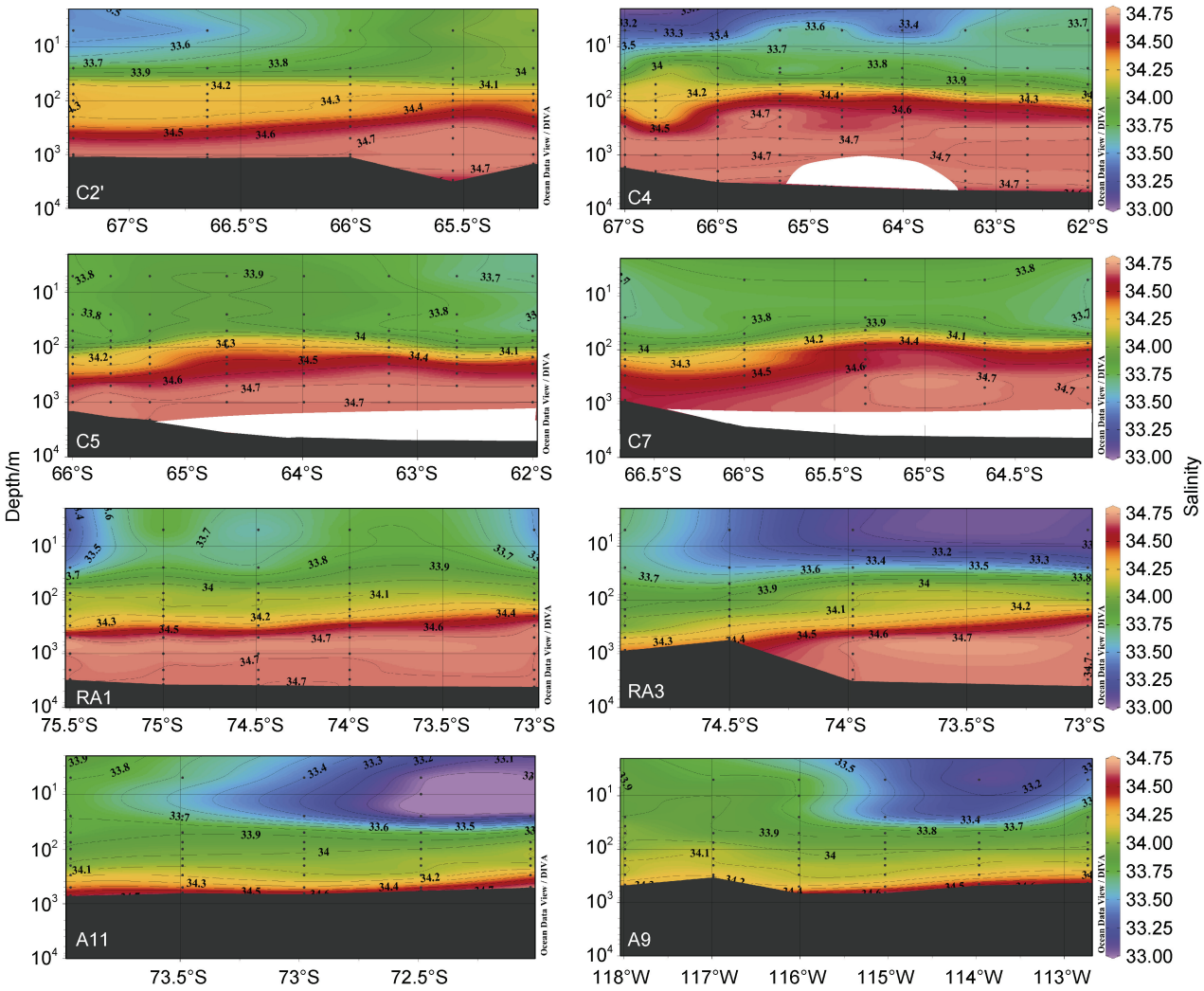


**Figure S6** Vertical distributions of salinity for the whole water depth along transects C2', C4, C5 and C7 in the Cosmonaut Sea and transects RA1, RA3, A11 and A9 in the Amundsen Sea.